Research article

# Adsorptive recovery of arsenic (III) ions from aqueous solutions using dried *Chlamydomonas* sp.

Mostafa Sh. Mohamed [a], Walaa G. Hozayen [a], Reem Mohammed Alharbi [c], Ibraheem Borie M. Ibraheem [b,*]

[a] Biochemistry Department, Faculty of Science, Beni-Suef University, Beni-Suef 62511, Egypt
[b] Botany and Microbiology Department, Faculty of Science, Beni-Suef University, Beni-Suef, 62511, Egypt
[c] Biology Department, Science College, University of Hafr Al Batin, Hafr Al Batin 39524, Saudi Arabia

ARTICLE INFO

ABSTRACT

The present study aimed to descry the effectiveness of dried microalga *Chlamydomonas* sp. for disposing of arsenic from aqueous solution. The study included examining the impact of some factors on algae's adsorption capacity (optimization study), such as initial concentrations of heavy metal, biosorbent doses, pH and contact time. All trials have been performed at constant temperature 25 °C and shaking speed of 300 rpm. The optimization studying indicated the pH 4, contact time at 60 min, temperature 25 °C and biomass concentration of 0.6 g/l were the best optimum conditions for the bioremediation activity with maximum removal percentage 95.2% and biosorption capacity 53.8 mg/g. Attesting of biosorption by applying FTIR (Fourier transfigure infrared), XRD (X-ray diffraction), SEM-EDX (Scanning Electron Microscope - Energy Dispersive X-ray), DLS (Dynamic light scarring) and ZP (Zeta Potential) was conducted. Also, Kinetics, isotherm equilibrium and thermodynamics were carried out to explain the plausible maximum biosorption capacity and biosorption rate of biosorbent q maximum.

## 1. Introduction

Metals are characterized by High electrical conductivity, malleability, and brilliance, which voluntarily give up their electrons to form cations. Metals are naturally present in the crust of the earth, and because their composition varies from place to place, there are spatial differences in the concentrations. The characteristics of the given metal and other environmental conditions are used to monitor the metal distribution in the atmosphere. The term "heavy metals" often refers to metals that have a particular density of more than 5 g/cm$^3$ and have a negative impact on the environment and living things (Jaishankar et al., 2014).

By the way, heavy metals cannot biodegrade and are divided into two categories. The first category consists of hazardous metals, such as Pb, Cd, and As, which are harmful, don't have any biological advantages for human health, and are poisonous at all doses. The second category consists of important metals, such as Cu, Zn, Mn, Fe, Ni, and Cr which are beneficial to human health biologically at low concentrations but poisonous at large doses (Abdel-rahman, 2022). Heavy metals risks affect negatively on both environment and humans. Hazardous heavy metals accumulate on plant cells thought absorption from soil which can't be

metabolized causing either damaging for plant cells or transformed to humans and animals during feeding. The side effects on humans causing by it varying according to heavy metal are ranging from redness of skin, GIT disorders, CNS damaging, liver necrosis and DNA damaging leading to tumors and cancers. The probabilities of these symptoms are directly proportional to heavy metal concentration and exposure time (Ali et al., 2019).

Exposure to heavy metals causes dangerous effects on human health. Arsenic is one of these heavy metals, and is very dangerous toxic element, whether it is trivalent or pentavalent forms causing hyperkeratosis and Skin lesions in hand. The inorganic trivalent forms such as arsenic trioxide, sodium arsenic and arsenic trichloride on the other hand the inorganic pentavalent forms such as arsenic pentoxide, arsenic acid, and arsenates such as lead arsenic (Tchounwou et al., 2012). Arsenic has been proven to be considered one of the biggest environmental dangers that put people's life in jeopardy of many people that live in multiple places, and the biogeochemical method has interacted to release natural arsenic into both surface and ground waters. Consequently, the exposition to arsenic mixes is the main danger concept to human health not only in developing communities but also in developed communities and dumping of arsenic
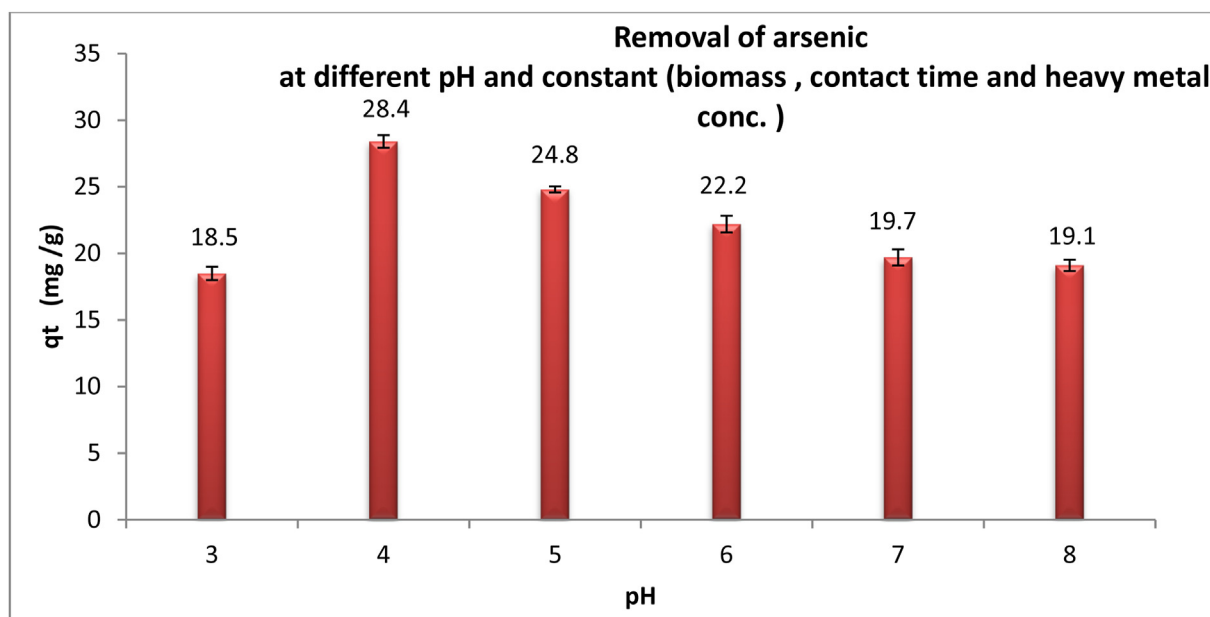
**Figure 1.** Effect of pH on biosorption of arsenic by the dried microalgae *Chlamydomonas* sp. at constant time 60 min, biosorbent dose 1 g/l, temperature 25 °C and heavy metal concentration 50 mg/l.
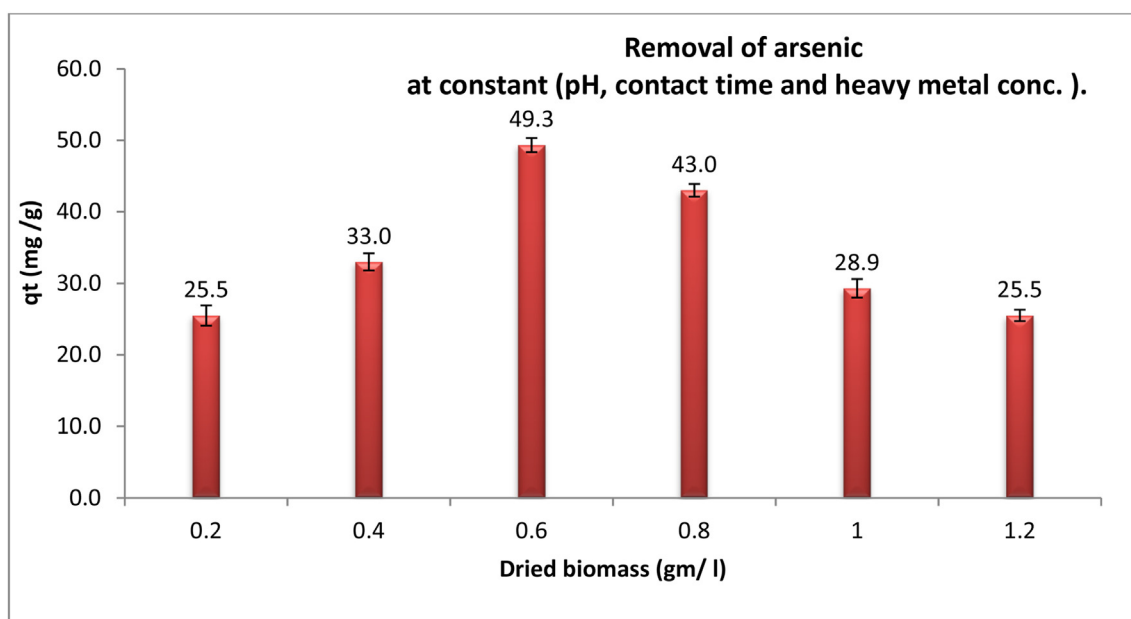


**Figure 2.** Effect of absorbent dosage (gm/l) on removal efficiency of arsenic by dried *Chlamydomonas* sp. at constant time 60 min, pH 4, temperature 25 °C and heavy metal concentration 50 mg/l.

from potable water is a worldwide priority (Mosaferi et al., 2014). The usual arsenic toxin can cause cardiovascular disease, high blood pressure and affect blood vessels.

According to Ladeira and Ciminelli (2004) the concentration of arsenic in industrial water can exceeds 100 mg/l and more due to some heavy metal industries so that he operates his study at initial arsenic concentration 1000 mg/l. The situation that reduced the maximum load for the detection of arsenic in drinking water from 50 to 10 mg/l and thus, more efficient water treatment processes are necessary to meet the new regulations (Hao et al., 2018). According to world health association (WHO), the maximum allowed limit of arsenic concentration in potable water is 0.01 mg/l.

Sources of heavy metals contamination are through Various industries such as fertilizer, mining, dyeing, polymers, plating, smelting, producing factories massively and widely result wastewaters containing many toxic substances, which after being transformed to rivers, underground water, lakes, agricultural lands and finally reach to living organisms and the human food chain (Peighambardoust et al., 2021).

Water is the most useful and basic natural resource on Earth. Indeed, though utmost corridor of the earth is enthralled with water clean water vacuity is getting scarcer in recent times. It has been prognosticated that in lower than 20 times, two – thirds of the world's population might face a freshwater deficit. The present script of adding water operation and global disposal will be the primary source of this unfavorable future. So
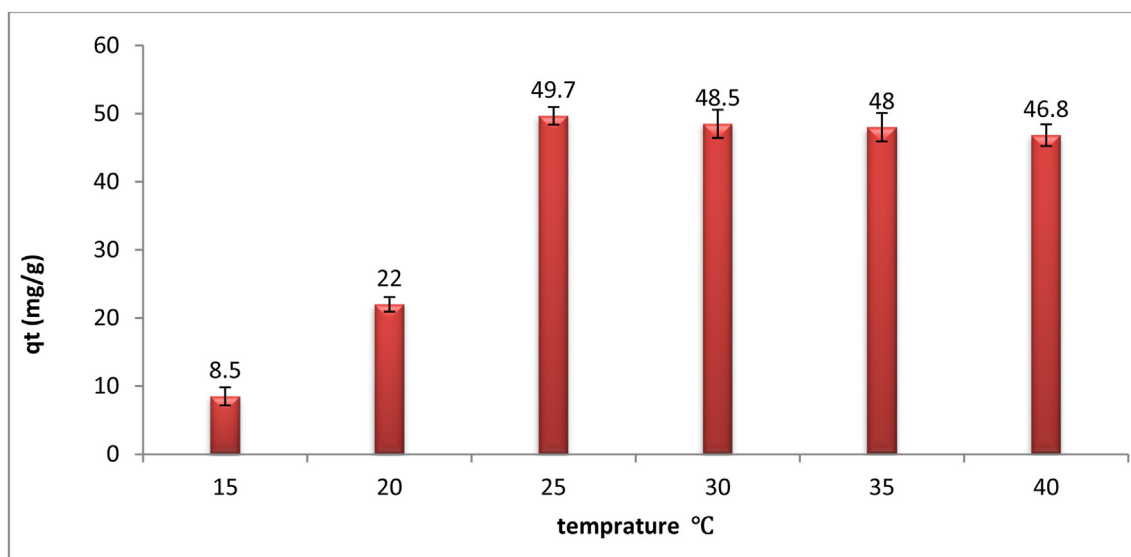
**Figure 3.** Effect of temprature on biosorption of arsenic by the dried microalgae *Chlamydomonas* sp. at pH 4, contact time 60 min, biosorbent dose 0.6 g/l, and heavy metal concentration 50 mg/l.

that humanity is in desperate need for extremity recycling of wastewater backwaters from human activates, husbandry, and artificial spots (Machineni, 2019).

Submarine ecosystem is substantially affected by heavy metal causing an implicit threat to living organisms and ecosystems. A biomagnification and accumulation of these element ions occur in food source. Although a trace of these elements is metabolically necessary to numerous living organisms, at advanced situations they can potentially be poisonous (Sibi, 2014).

Considering the arsenic impurity in groundwater, arsenic is found in water sources mainly in the As (III), (arsenite) and As (V) (arsenate) oxidation states. Arsenic may could be detected both inorganic and organic components in water. Inorganic forms (arsenite and arsenate) are the most species that are frequently determined, and these are more toxic than organic species (Fazal et al., 2001).

Any favorable treatment procedure of arsenic defiled water has to get rid of both As (V) and As (III) forms but occasionally usual. Technologies aren't effective enough in the junking of As (III). for illustration, the most common treatment technologies frequently bear peroxidation of As (III) to As (V) as As (III) is more delicate to remove by the appreciatively charged shells of adsorbent so the focus of this study is how to get relieve of As (III) so that natural treatment of heavy essence defiled water are more respectable affordable and gainful (Cavalca et al., 2013).

There are several method carried out to remove heavy metals from polluted water as Chemical Precipitation, Chemical Oxidation and Reduction, Membrane Separation, Ion Exchange and Ultrasonic Removal of Heavy Metals. And all of these ways have benefits and disadvantage. The selected method based on the usage of treated water and the degree of its pollution (Nalenthiran et al., 2016). In this issue, the adsorption mechanism is more affordable compared to the other methods due to its benefits such as high efficacy, simplicity, high regeneration, compliance adsorbent dose, reuse performance and low risk (Foroutan et al., 2022). Surface adsorption by activated carbon is a potent technique used to recover and remove heavy metal ions from industrial wastewaters. Due to its high manufacturing costs and reliance on non-renewable resources, activated carbon has recently been ignored. As a result, the biosorption procedure is the best option for treating the bulk wastewater. To date, a wide variety of bioadsorbents, including bacteria, algae, fungi, and yeast, have been employed for the biosorption of heavy metal ions (Naeimi et al., 2018).

Primitive and eukaryotic algae are organisms that live in all water sources with a superior ability to remove heavy metals, as they are considered environmentally friendly natural sources, and they can live in water polluted with these minerals (Hammouda et al., 2015; Singh et al., 2016; Al-Homaidan et al., 2018). Several studies have indicated the positive use of algal organisms, both those that live in freshwater and those that proliferate in saltwater, that they can remove hazardous heavy metals in water bodies (Ayangbenro and Babalola, 2017; Ubando et al., 2020). Microalgae can resist heavy metal poisoning by two mechanisms, the adsorption mechanism on the outside of cells and the intracellular adsorption mechanism due to attraction between negatively charged functional group on microalgae surface and heavy metal cations (Petrovïc and Simonïc, 2016; Dulla et al., 2020). The biosorption of lethal ions to microalgal cell-walls was conducted (Kumar et al., 2015). A recent approved study also demonstrated the ability of two types of microalgae, *Phormidium tenue* and *Chlorella vulgaris*, as bio-sorbent materials to remove cobalt from aqueous solutions (Abdel-Raouf et al., 2022).

The target of our work article was to determine the efficacy of the dry biomass for freshwater microalga *Chlamydomonas* sp. in getting rid of arsenic (III) from watery solution and the effects of various chemicals environmental conditions to increase this efficiency. Factor affecting on adsorption equilibrium mechanism as pH, initial concentration, adsorbent dose, contact time and temperature were obtained. The structural and morphological composition of adsorbent was studied using FTIR, XRD, SEM, DLS and ZP. Characterization as Kinetic, isothermal and thermodynamic studies carried out (Foroutan et al., 2021a). The advantage of this study is bioremoving of arsenic (III) at high concentrations up to 100 mg/l in short time plus excellence reusability of biosorbent in comparison with previous studies. But more than 100 mg/l the bioremoving isn't effective.

## 2. Materials and methods

### 2.1. Preparation of biosorbent

In this study, biosorbent microalga *Chlamydomonas* sp. was kindly supplied from the Phycological Laboratory, Faculty of Science, Beni-Suef University, followed by re-subculture in suitable growth media (BG11 medium) to get an intensive biomass production sufficient for metal binding experiment (Rippka, 1988). Collected biomass was dried at 50 °C till complete dryness (El-Awamri et al., 2015) (supporting data, Figure S1). Next, the grind dried biomass well to get fine powder with uniform particle size to increase biosorption capacity (Kashyap et al., 2019).
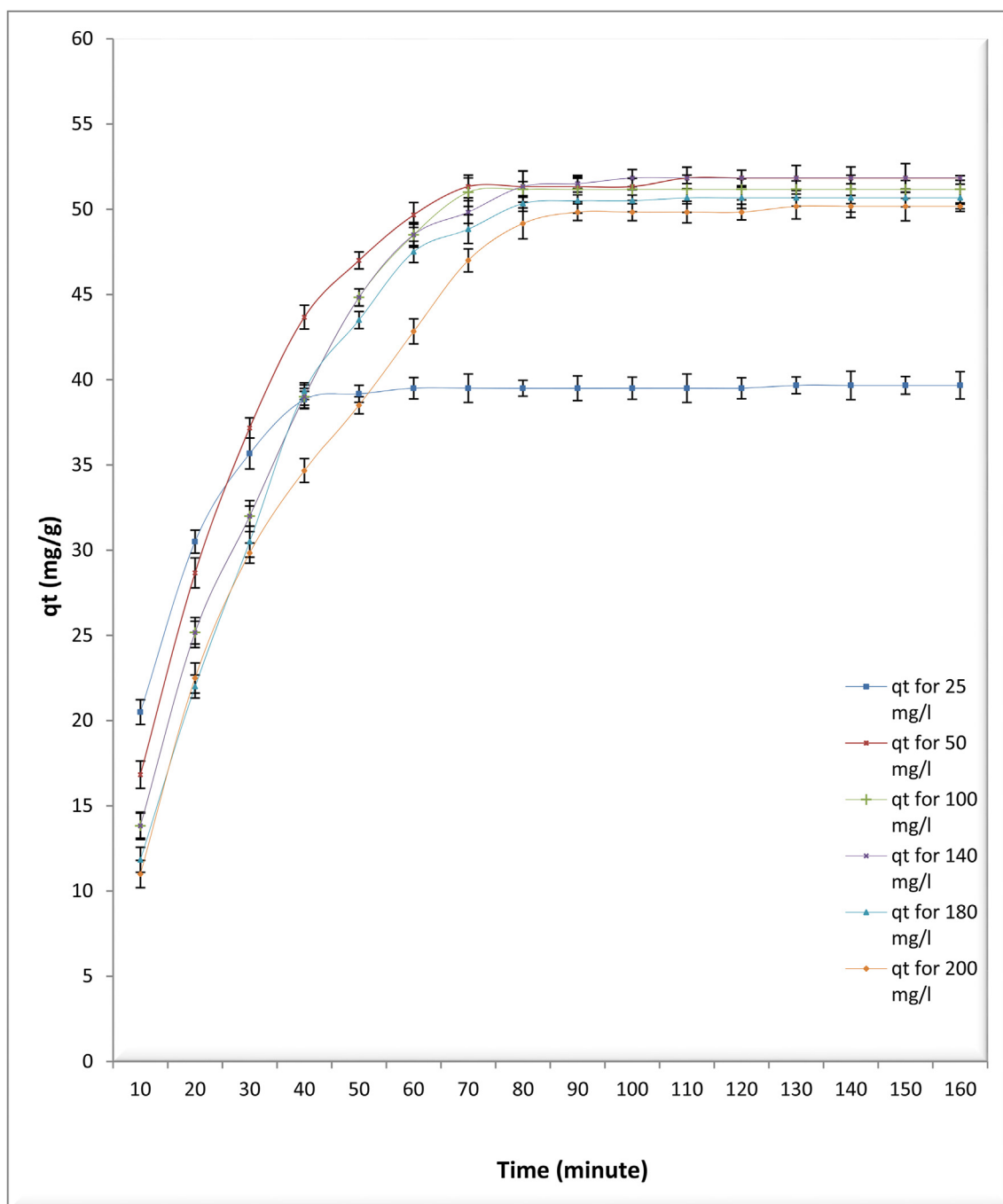
**Figure 4.** Investigating the effect of contact time interval from 10 to 160 min on biosorption capacity for different concentrations of arsenic (mg/l) by dried *Chlamydomonas* sp. at pH 4, temperature 25 °C and biosorbent 0.6 g/l.

## 2.2. Preparation of arsenic

Sodium arsenite (NaAsO₂) was attained from (Fischer Chemicals). Stock results (1000 mg/l) of As (III) were attended by dissolving applicable quantities 1.751 g of (NaAsO₂), in 1000 ml distilled deionized (DI) water. Results of needed lower concentration were prepared by lacing the stock results (Boddu et al., 2008). The pH was adjusted by NaOH (0.1 M) and HCl (0.1 M).

## 2.3. Biosorption experiments (factors affecting the biosorption process)

After adjusting the pH of desired concentration of arsenic aqueous solution through NaOH and HCl a batch model is attended by adding 100 ml of arsenic solution in a 250 ml Erlenmeyer flask. Then a favorable weight of biosorbent added to the solution all flasks are fixed to shaker at speed 300 rpm. After detected time flasks are rested for minutes at room temperature by centrifugation for 5 min at 3000 rpm speed to get supernatant which was measured by ICP to determine the residual arsenic concentration and by the following calculating removal efficacy percentage % and biosorption capacity $q_t$. To investigate optimum pH of biosorption process at constant initial heavy metal concentration, biomass weight and contact time. Adjusting pH values of heavy metal aqueous solution are (3, 4, 5, 6,7 and 8) through NaOH (0.1 M) and HCl (0.1 M) (Ibrahim et al., 2016). Biosorbent dosage in the solution is a crucial parameter effecting metal adsorption. we make the sequence of biosorbent doses (0.2, 0.4, 0.6, 0.8, 1, and 1.2 g/l) to detect the degree of

**Table 1.** Effect of contact time on biosorption capacity at variable arsenic (III) concentration, constant pH 4 and constant dried biomass 0.6 g/l.

| t (minute) | Removal percentage (%) for 25 mg/l | q$_t$ for 25 mg/l | ±SD | Removal percentage (%) for 50 mg/l | q$_t$ for 50 mg/l | ±SD | Removal percentage (%) for 100 mg/l | q$_t$ for 100 mg/l | ±SD | Removal percentage (%) for 140 mg/l | q$_t$ for 140 mg/l | ±SD | Removal percentage (%) for 180 mg/l | q$_t$ for 180 mg/l | ±SD | Removal percentage (%) for 200 mg/l | q$_t$ for 200 mg/l | ±SD |
|---|---|---|---|---|---|---|---|---|---|---|---|---|---|---|---|---|---|---|
| 10 | 49.2 | 20.5 | 0.04 | 20.2 | 16.83 | 0.06 | 8.3 | 13.83 | 0.05 | 5.93 | 13.83 | 0.19 | 3.94 | 11.83 | 0.03 | 3.3 | 11.00 | 0.97 |
| 20 | 73.2 | 30.5 | 0.16 | 34.4 | 28.66 | 0.02 | 15.1 | 25.17 | 0.12 | 10.79 | 25.167 | 0.45 | 7.33 | 22 | 0.10 | 6.75 | 22.50 | 0.59 |
| 30 | 85.6 | 35.66 | 0.16 | 44.6 | 37.17 | 0.11 | 19.2 | 32.00 | 0.11 | 13.71 | 32 | 0.10 | 10.17 | 30.5 | 0.00 | 8.95 | 29.83 | 0.09 |
| 40 | 93.2 | 38.83 | 0.19 | 52.4 | 43.67 | 0.12 | 23.4 | 39.00 | 0.27 | 16.71 | 39 | 0.20 | 13.11 | 39.33 | 0.35 | 10.4 | 34.67 | 0.01 |
| 50 | 94 | 39.16 | 0.28 | 56.6 | 47.00 | 0.23 | 26.9 | 44.83 | 0.29 | 19.21 | 44.83 | 0.10 | 14.50 | 43.5 | 0.90 | 11.55 | 38.50 | 0.08 |
| 60 | 94.8 | 39.5 | 0.12 | 59.6 | 49.67 | 0.14 | 29.1 | 48.50 | 0.15 | 20.79 | 48.5 | 0.91 | 15.83 | 47.5 | 0.06 | 12.85 | 42.83 | 0.07 |
| 70 | 94.8 | 39.5 | 0.04 | 59.6 | 51.33 | 0.20 | 30.6 | 51.00 | 0.08 | 21.36 | 49.83 | 0.34 | 16.44 | 48.83 | 0.04 | 14.1 | 47.00 | 0.14 |
| 80 | 94.8 | 39.5 | 0.15 | 59.6 | 51.33 | 0.10 | 30.7 | 51.17 | 0.14 | 22.00 | 51.33 | 0.96 | 17.39 | 50.33 | 0.05 | 14.75 | 49.17 | 0.13 |
| 90 | 94.8 | 39.5 | 0.09 | 59.6 | 51.33 | 0.23 | 30.7 | 51.17 | 0.20 | 22.07 | 51.5 | 0.33 | 17.39 | 50.5 | 0.09 | 15.95 | 49.83 | 0.03 |
| 100 | 94.8 | 39.5 | 0.01 | 60.2 | 51.33 | 0.01 | 30.7 | 51.17 | 0.31 | 22.21 | 51.83 | 0.07 | 17.39 | 50.5 | 0.12 | 15.95 | 49.83 | 0.55 |
| 110 | 94.8 | 39.5 | 0.01 | 60.2 | 51.83 | 0.02 | 30.7 | 51.17 | 0.23 | 22.21 | 51.83 | 0.23 | 17.39 | 50.67 | 0.62 | 15.95 | 49.83 | 0.64 |
| 120 | 94.8 | 39.5 | 0.01 | 60.2 | 51.83 | 0.01 | 30.7 | 51.17 | 0.02 | 22.21 | 51.83 | 0.01 | 17.72 | 50.67 | 0.09 | 16.15 | 49.83 | 0.63 |
| 130 | 95.2 | 39.66 | 0.01 | 60.6 | 51.83 | 0.11 | 30.7 | 51.17 | 0.01 | 22.21 | 51.83 | 0.02 | 17.72 | 50.67 | 0.76 | 16.15 | 50.17 | 0.07 |
| 140 | 95.2 | 39.66 | 0.02 | 60.6 | 51.83 | 0.02 | 30.7 | 51.17 | 0.02 | 22.21 | 51.83 | 0.43 | 17.72 | 50.67 | 0.09 | 16.15 | 50.17 | 0.54 |
| 150 | 95.2 | 39.66 | 0.32 | 60.6 | 51.83 | 0.48 | 30.7 | 51.17 | 0.23 | 22.21 | 51.83 | 0.63 | 17.72 | 50.67 | 0.01 | 16.15 | 50.17 | 0.09 |
| 160 | 95.2 | 39.66 | 0.04 | 60.6 | 51.83 | 0.13 | 30.7 | 51.17 | 0.14 | 22.21 | 51.83 | 0.80 | 17.72 | 50.67 | 0.76 | 16.15 | 50.17 | 0.02 |

*Where t is time (minute), q$_t$ is biosorption capacity at certain time (mg/g) and SD is standard deviation.

**Table 2.** Values of 1st order kinetic models.

| initial conc. (mg/l) | intercept | slope | q$_{max}$ measured (mg/g) | q$_{max}$ (mg/g) | R$^2$ | k$_1$ |
|---|---|---|---|---|---|---|
| 25 | 3.81 | -0.0878 | 39.67 | 45.45 | 0.9965 | -0.023 |
| 50 | 4.27 | 0.064 | 51.83 | 71.87 | 0.9801 | 0.014971 |
| 100 | 4.33 | 0.0522 | 51.17 | 75.99 | 0.956 | 0.012054 |
| 140 | 4.38 | 0.0539 | 51.83 | 80.17 | 0.9722 | 0.012294 |
| 180 | 4.25 | -0.0433 | 50.67 | 70.25 | 0.9906 | -0.01018 |
| 200 | 4.17 | 0.0324 | 50.17 | 62.71 | 0.9796 | 0.007829 |

*Where q$_{max}$ is biosorption capacity (mg/g). K$_1$ is the pseudo-first-order rate constant for the kinetic model (1/min) and R$^2$ is the regression correlation coefficients.

effect of biosorbent dose in biosorption capacity at optimum pH, initial concentration, and contact time (Kahraman et al., 2005). Preparing sequence of heavy metal concentrations (25, 50, 100, 140, 180 and 200 mg/l) of arsenic at constant contact time, biosorbent dose and optimum pH apply batch system to monitoring initial concentration effect of arsenic on the biosorption capacity's effectiveness (Kumar et al., 2020).

Temperature is a critical and important parameter in the adsorption process. Sequences of biosorption experiments carried out win in range (15, 20, 25, 30, 35, and 40 °C) at constant pH, dried biomass, contact time and initial heavy metal concentration (Olukanni et al., 2014). Measuring biosorption capacity at several times during procedure at constant biosorbent dose and optimum pH variation of contact time was applied to the arsenic concentration desired of the solution which yielded the maximum biosorption capacity and efficiency (Alpat et al., 2010).

The effect of common inorganic ions such as Na$^+$, K$^+$, Ca$^{2+}$ ions on the biosorption was carried out for arsenic (III) at optimum conditions with constant initial metal concentration 50 mg/l and varying in concentration for each inorganic ion (20, 40, 60, 80 and 120 mg/l). By ending the biosorption experiments the residual arsenic detected by ICP to calculate biosorption capacity q$_t$ and removal percent %.

### 2.4. Biomass characterization

Enables to identify chemical groups exist on the surface of *Chlamydomonas* sp. was detected by **FTIR** (Bruker Vertex 70, OPUS version 7.2 build: 7, 2, 139, 139, 1294 20130108, USA). Spectra were measured in the 4000 cm$^{-1}$ to 400 cm$^{-1}$ wavenumber ranges with scans collected at 4 cm$^{-1}$ resolutions. **Powder X-Ray Diffraction**. X-ray diffraction was performed on Desktop X-ray Diffractometer Rigaku, MiniFlex II. Samples were analyzed in angular range of 2 theta (10°–90°). **Scanning electron microscopy Analysis**, the pre and post biosorption process biosorbent were analyzed by SEM-EDX with this mechanism, a clear and pure image were diagnosed that make it can examine the morphological features along with the elemental analysis of the surface pre and post the biosorption operation.

The apparatus model is (JSM-6510LA SERIES 18, JAPAN). **Dynamic light scarring (DLS)** shows particle size of dried biomass and its uniformity which illustrate investigation and accuracy of biosorption process. **ZP (zeta potential)** is suitable technique for detection biomass surface charge and its effect by pH value therefore biosorption capacity it was applied by (ZETASIZER, MALVERN, UK).

### 2.5. Biosorption kinetic study

The results of all trials should be replicated thrice and were equaled arsenic bioremoval percentage it was calculated for each one Eq. (1) by following expression:

$$R\% = ((C_i - C_e)/C_i) \times 100 \tag{1}$$

**Table 3.** Values of 2nd order kinetic models.

| initial conc. (mgl$^{-1}$) | intercept | slope | q max measured (mg/g) | q max (mg/g) | q max$^2$ | k$_2$ | R$^2$ |
|---|---|---|---|---|---|---|---|
| 25 | 0.3082 | 0.0177 | 39.67 | 56.49 | 3191.931 | 0.001017 | 0.9992 |
| 50 | 0.4699 | 0.0115 | 51.83 | 86.96 | 7561.437 | 0.000281 | 0.9473 |
| 100 | 0.6101 | 0.0103 | 51.17 | 97.09 | 9425.959 | 0.000174 | 0.989 |
| 140 | 0.5651 | 0.0115 | 51.83 | 86.96 | 7561.437 | 0.000234 | 0.9923 |
| 180 | 0.7088 | 0.0094 | 50.67 | 106.38 | 11317.34 | 0.000125 | 0.954 |
| 200 | 0.7203 | 0.0111 | 50.17 | 90.09 | 8116.224 | 0.000171 | 0.9767 |

*Where qmax is biosorption capacity (mg/g), K2 is the 2nd order rate constant for the kinetic model (g mg$^{-1}$ min$^{-1}$) and R2 is the regression correlation coefficients.

**Table 4.** Values of elovich kinetic models.

| Initial conc. (mg/l) | slope | inter | β (g/mg$^{-1}$) | α (mg g$^{-1}$ min$^{-1}$) | R2 |
|---|---|---|---|---|---|
| 25 | 11.338 | -3.8857 | 0.088198977 | 8.04817334 | 0.999 |
| 50 | 24.216 | -48.945 | 0.041295012 | 3.208582436 | 0.9473 |
| 100 | 19.476 | -32.312 | 0.051345245 | 3.706601311 | 0.9899 |
| 140 | 19.051 | -30.641 | 0.052490683 | 3.81428252 | 0.9929 |
| 180 | 20.213 | -36.375 | 0.049473111 | 3.342575227 | 0.9874 |
| 200 | 18.375 | -32.232 | 0.054421769 | 3.17995993 | 0.9954 |

*Where β is desorption constant (g/mg$^{-1}$), α is the initial adsorption rate (mg g$^{-1}$ min$^{-1}$) and R2 is the regression correlation coefficient.

**Table 5.** Values of intraparticle diffusion kinetic models.

| initial conc (mg/l) | k$_{diff}$ (mg g$^{-1}$·min$^{-0.5}$) | intercept | R$^2$ |
|---|---|---|---|
| 25 | 6.6051 | 0.021 | 0.9888 |
| 50 | 0.1253 | 0.9522 | 0.9909 |
| 100 | 7.6192 | -9.6079 | 0.9903 |
| 140 | 7.0341 | -6.3991 | 0.9865 |
| 180 | 7.4687 | -10.688 | 0.9825 |
| 200 | 6.4876 | -7.3784 | 0.9903 |

*Where Kdiff is intraparticle diffusion constant (mg g$^{-1}$ min$^{-0.5}$), R2 is the initial adsorption rate (mg/g. min) and R2 is the regression correlation coefficient.

where Ce and Ci we were representing the residual and the initial concentrations of arsenic in the aqueous solution respectively and R is bioremoval percentage. The bioremoval capacity of biosorbent which is observed from the weight balance on the sorbet in a batch system with solution volume v is used to acquire the method biosorption isotherms within the method conditions. The bioremoval capacity of microalgae for each of arsenic concentration at equilibrium was counted through Eq. (2).

$$qe \text{ (mg/g)} = ((Ci - Ce)/M) \tag{2}$$

where qe is biosorption capacity at equilibrium, Ce resembles the residual arsenic concentration, Ci resembles the initial arsenic concentration in an aqueous solution in (mg/l). V resembles the aqueous solution volume in (L) and M is the weight of adsorbent in (gm) used.

To demonstrate the symbolic differences in the kinetic rates and explain the kinetic bioremoval of arsenic, the mentioned models of first and pseudo-second-order were used the direct form of the both models as Eqs. (3) and (4) respectively.

$$\ln [qe - qt] = \ln qe - k_1 t \tag{3}$$

$$t/qt = t/qe + 1/(k_2 qe^2) \tag{4}$$

where ln is logarithm qe represent the equilibrium biosorption capacity (mg/g) and $k_1$ refers to the kinetic rate constant (min$^{-1}$), $K_2$ is pseudo-second kinetic rate constant (g mg$^{-1}$ min$^{-1}$), q$_t$ is the amount of

biosorption quantity (mg/g) at time t, q is biosorption capacity. The kinetic model formula of Elovich was mainly elevated to illustrate kinetics mechanism of gases chemisorption onto solids has lately used adding mapping to demonstrate the expected kinetics for kinetics of certain adsorbents in aqueous phase onto adsorbents (Zand and Abyaneh, 2020). This kinetic model has resembled as follows Eq. (5).

$$qt = 1/β \ln (1 + α β t) \tag{5}$$

where qt is biosorption capacity at certain time (mg/g), ln is logarithm, α is initial biosorption rate (mg g$^{-1}$ min$^{-1}$), β is the desorption constant (mg/g), t is time. From intercept and slope of plotting the linear graph of qt versus ln t, the constants can be obtained. The pseudo-second-order kinetic model demonstrates the overall adsorption kinetics, but it doesn't provide suitable knowledge about the control rate of adsorption mechanism steps (Liao et al., 2010). Therefore, the intraparticle model is crucial in illustrating biosorption of arsenic by dried microalgae, In conformity with this model, the graph carried out by plotting uptake (qt), versus the square root of time (t$^{0.5}$) as shown is Eq. (6).

$$qt = (k_{diff} \times t^{0.5}) + C \tag{6}$$

where qt is biosorption capacity (mg/g), Kdiff is the intraparticle diffusion rate constant (mg g$^{-1}$·min$^{-0.5}$), t is time (min) and C is intercept.

### 2.6. Biosorption isotherm models

Both Langmuir and Freundlich isotherms possess the necessary abilities to predict the behavior of adsorption equilibrium. Therefore, the removal of metals by the dried biomass can be impacted by these two isotherms models added to other isothermic models as Temkin and Dubinin – Radushkevich. That is, parts of the adsorbent surface might have a monolayer and homogeneous adsorption, and other parts might be homogeneous and multilayer (Foroutan et al., 2021b). The relation at a constant temperature among the whole biosorbed quantity of substance per unit mass of biosorbent and its equilibrium concentration is known as isotherm adsorption it usually provides crucial data in enhancing biosorbent utilization Freundlich and Langmuir models are widely used in characterizing isotherms of biosorption and provide important parameters to predict adsorption efficiency (Korake and Jadhao, 2021). Freundlich and Langmuir isotherm is the most used model to estimate data mining.

Langmuir isotherm model:

Langmuir isotherm is used to illustrate monolayer sorption onto the surface of a biosorbent with a limited number of identical biosorption sites and no interaction between sites (Mittal et al., 2007). The model is expressed as Eq. (7).

$$Ce/qe = 1/(q_{max} b) + Ce/q_{max} \tag{7}$$

where Ce is heavy metal concentration at equilibrium, qe is biosorption capacity at equilibrium (mg/g), b (L/mg) is the equilibrium constant related to the adsorption energy, and q$_{max}$ is the maximum adsorption

**Table 6.** Calculated values for plotting langmuir and freundlich isotherm model.

| Exp. no. | Ci (mg/l) | Ce (mg/l) | qe (mg/g) | 1/Ce | ln Ce | Ce/qe | 1/qe | log qe | log Ce | R (J/mol k) | Ln qe | T+273.15 | 1+(1/Ce) | ln(1+(1/ce)) | RTln1+(1/Ce) | $\varepsilon^2$ |
|---|---|---|---|---|---|---|---|---|---|---|---|---|---|---|---|---|
| 1 | 25 | 1.7 | 38.83333 | 0.58824 | 0.530628 | 0.043777 | 0.025751 | 1.589205 | 0.230449 | 8.314 | 3.659279 | 262.15 | 1.58823529 | 0.46262352 | 1008.294952 | 1016658.71 |
| 2 | 50 | 20.2 | 49.66667 | 0.0495 | 3.005683 | 0.406711 | 0.020134 | 1.696065 | 1.305351 | 8.314 | 3.905334 | 262.15 | 1.04950495 | 0.04831858 | 105.3110688 | 11090.42121 |
| 3 | 100 | 69.4 | 51 | 0.01441 | 4.239887 | 1.360784 | 0.019608 | 1.70757 | 1.841359 | 8.314 | 3.931826 | 262.15 | 1.01440922 | 0.0143064 | 31.18100535 | 972.2550945 |
| 4 | 140 | 109.2 | 51.43333 | 0.00916 | 4.693181 | 2.123137 | 0.019443 | 1.711245 | 2.038223 | 8.314 | 3.940286 | 262.15 | 1.00915751 | 0.00911583 | 19.86809656 | 394.741261 |
| 5 | 180 | 148.7 | 52.16667 | 0.00672 | 5.001931 | 2.850479 | 0.019169 | 1.717393 | 2.172311 | 8.314 | 3.954444 | 262.15 | 1.00672495 | 0.00670244 | 14.60806474 | 213.3955554 |
| 6 | 200 | 168.1 | 53.16667 | 0.00595 | 5.124559 | 3.161755 | 0.018809 | 1.725639 | 2.225568 | 8.314 | 3.973432 | 262.15 | 1.00594884 | 0.00593122 | 12.92717372 | 167.1118204 |

*Where Ci is initial heavy metal concentration (mg/l), Ce is heavy metal concentration at equilibrium (mg/l), R is the universal gas constant (mg/l), $\varepsilon^2$ is square of potential energy and qe is biosorption capacity at equilibrium (mg/g).

capacity (mg/g). The parameters of Langmuir isotherm were obtained by plotting Ce/qe versus Ce.

Freundlich isotherm model:

The linear form of Freundlich isotherm equation is given as Eq. (8).

$$\text{Log } q_e = \log k_F + (1/n) \log C_e \tag{8}$$

where qe is the amount biosorbed substance in the biosorbent (mg/g), Ce is the equilibrium concentration of biosorbate in solution (mg/l), and kf (mg/g) is the Freundlich constants depending on the temperature and the given biosorbent-biosorbate couple. $1/n$ is the heterogeneity factor; n is a measure of the deviation from linearity of adsorption (gm/l) (Fan et al., 2016). The parameters of Freundlich isotherm were obtained by plotting log qe versus log Ce.

The Temkin Isotherm model:

This isotherm model has a function that clearly accounts for the interactions between the adsorbent and adsorbate. The model assumes that the heat of adsorption (function of temperature) of all molecules in the layer would drop linearly rather than logarithmically with coverage by ignoring the extremely low and high value of concentrations (Dada et al., 2012). The graph is plotted between $q_e$ against $\ln c_e$. Temkin model is expressed as the following Eqs. (9), (10), and (11):

$$B = RT/b_T \tag{9}$$

$$K_T = \text{EXP (intercept/B)} \tag{10}$$

$$q_e = B \ln A_T + B \ln C_e \tag{11}$$

where $A_T$ is Temkin isotherm equilibrium binding constant (l/g), $K_T$ is Temkin isotherm constant (l/mg), R is universal gas constant (8.314 J/mol K), T is Temperature at 298 K and B is Constant related to heat of sorption (J/mol).

Dubinin-Radushkevich isotherm model:

This isotherm model was detected to investigate the characteristic porous properties of the biomass and the apparent energy of adsorption (Foroutan et al., 2021c). The graph is plotted between $\ln q_e$ against $\varepsilon^2$. The model is expressed by the following Eqs. (12), (13), and (14):

$$\varepsilon = RT \ln (1 + 1/C_e) \tag{12}$$

$$q_e = q_m \exp (-k\varepsilon^2) \tag{13}$$

$$\ln q_e = \ln q_m - K\varepsilon^2 \tag{14}$$

where $C_e$ is concentration at equilibrium (mg/l), $q_e$ is adsorption capacity at equilibrium (mg/g), $q_m$ adsorption capacity (mg/g), K is D-R isotherm constant (mol²/kj²), $\varepsilon$ is adsorption potential, R is universal gas constant (8.314 J/mol K), T is temperature in kelvin (k) and E is energy (KJ/mol).

### 2.7. Thermodynamic studies

Thermodynamic parameters including the change in free enthalpy (ΔH°), energy (ΔG°), and entropy (ΔS°) were detected to explain thermodynamic behavior of the biosorption of As (III) ions. The graph is detected through plotting $1/T$ versus $\ln K$ (Spain et al., 2020). These parameters were calculated according to the following Eqs. (15), (16), (17), (18), (19), and (20):

$$K = q_e/C_e \tag{15}$$

$$\Delta H° = -\text{slop} \times R \tag{16}$$

$$\Delta S° = \text{intercept} \times R \tag{17}$$

**Table 7.** R2 and constants for Langmuir, Freundlich, Temkin and Dubinin-Radushkevich isotherm models.

| Langmuir | | | Freundlich | | | Temkin | | | Dubinin–Radushkevich | | | |
|---|---|---|---|---|---|---|---|---|---|---|---|---|
| $q_{max}$ (mg/g) | $K_L$ (l/mg) | $R^2$ | $k_f$ (mg/g) | 1/n | $R^2$ | $k_t$ (l/mg) | B (J/mol) | $R^2$ | $q_{max}$ (mg/g) | E (KJ/mol) | $k_{DR}$ (mol$^2$/kj$^2$) | $R^2$ |
| 52.9100529 | 0.6 | 0.9995 | 37.00837363 | 0.0641 | 0.9274 | 1.88 | 2.9132 | 0.9381 | 51.5 | 1290.9 | 3.00E-07 | 0.9655 |

*Where $q_{max}$ is the maximum adsorption capacity (mg/g), KL is Langmuir constant (l/mg), Kf is Freundlich constant (mg/g), kt is Temkin constant (l/mg), kDR is Dubinin–Radushkevich isotherm constant(mol$^2$/kj$^2$), 1/n is the empirical constant, R2 is the regression correlation coefficient and E is energy of adsorption.
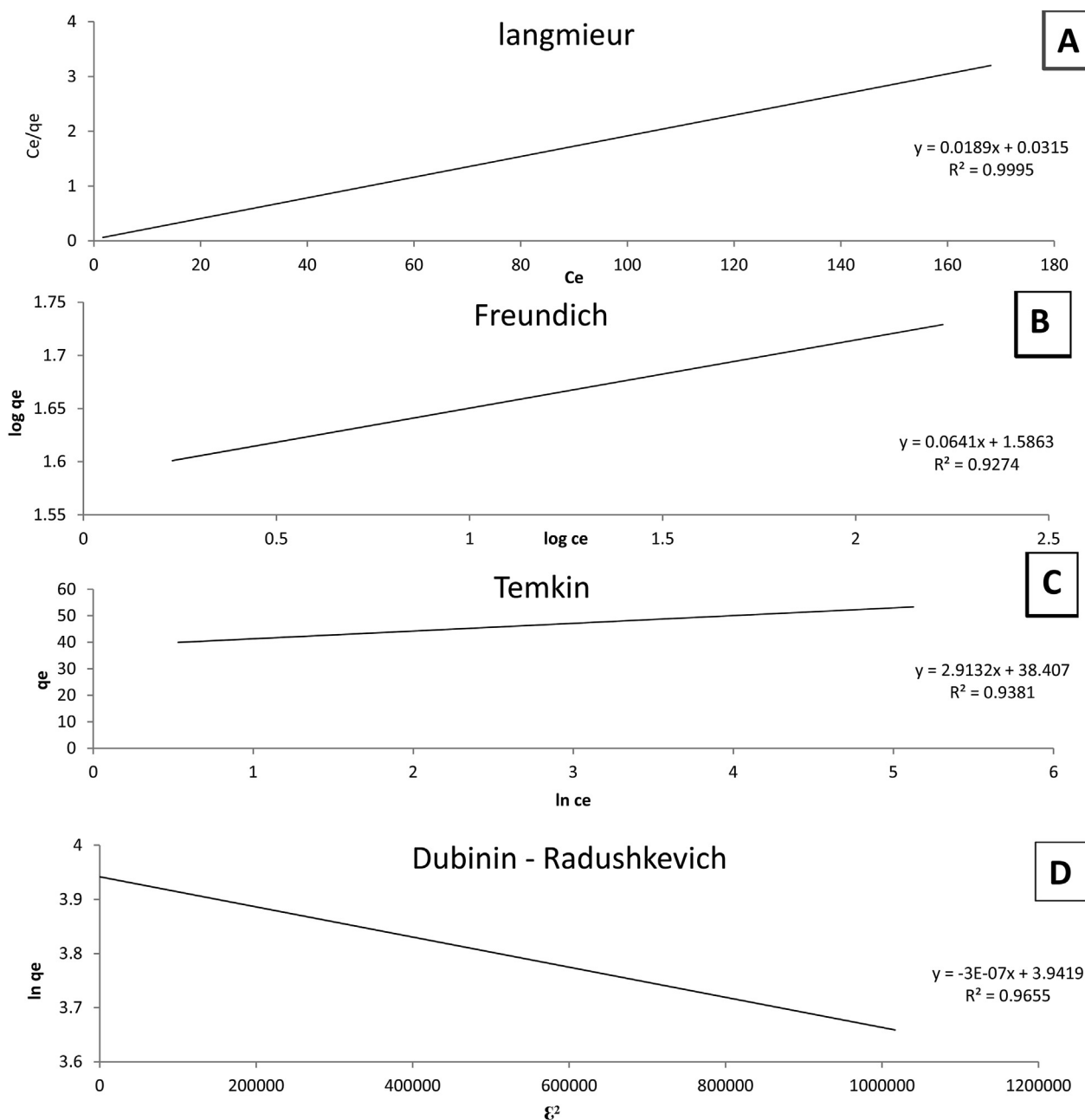


**Figure 5.** Isotherm models for As(III) biosorption (A) Langmuir, (B) Freundlich, (C) Temkin and (D) Dubinin-Radushkevich.

$$\Delta G° = -RT \ln k \quad\quad (18)$$

$$\Delta G° = \Delta H - T\Delta S° \quad\quad (19)$$

$$\ln K = (\Delta S°/R) - (\Delta H°/RT) \quad\quad (20)$$

where R is the universal gas constant (8.314 J/mol K), T is temperature (K) and K is the distribution coefficient. ($\Delta G°$) is energy (KJ mol$^{-1}$), ($\Delta H°$) the enthalpy (KJ mol$^{-1}$), and ($\Delta S°$) entropy (JK$^{-1}$ mol$^{-1}$), the biosorption were estimated from the slope and intercept of the plot of ln $K_L$ versus 1/T.
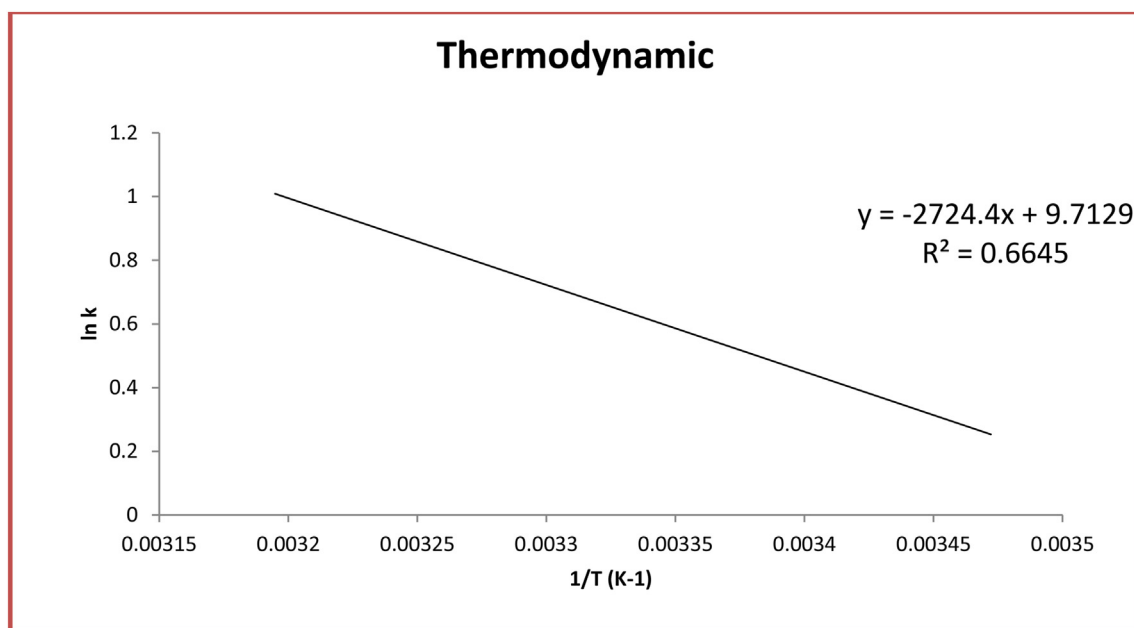
**Figure 6.** Thermodynamic graph explain the effect of temprature (15, 20, 25, 30, 35 and 40 °C) on biosorption of arsenic by the dried microalgae *Chlamydomonas* sp. at pH 4, contact time 60 min, biosorbent dose 0.6 g/l, and heavy metal concentration 50 mg/l.

**Table 8.** Values of thermodynamic study.

| t °C | T (K) | K (K$^{-1}$) | ΔG° (KJ mol$^{-1}$) | ΔH° (KJ mol$^{-1}$) | ΔS° (JK$^{-1}$ mol$^{-1}$) | R$^2$ |
|------|-------|--------------|---------------------|---------------------|----------------------------|-------|
| 15 | 288 | 1.106162 | -0.241589144 | 22.65053307 | 80.75271804 | 0.6645 |
| 20 | 293 | 1.349638 | -0.730401515 | | | |
| 25 | 298 | 2.458746 | -2.22895115 | | | |
| 30 | 303 | 2.376396 | -2.180531171 | | | |
| 35 | 308 | 2.342767 | -2.180018208 | | | |
| 40 | 313 | 2.267884 | -2.130871799 | | | |

* Where T is temperature (K) and K is the distribution coefficient, (ΔG°) is energy (KJ mol$^{-1}$), (ΔH°) the enthalpy (KJ mol$^{-1}$), (ΔS°) entropy (JK$^{-1}$ mol$^{-1}$) and R2 is the regression correlation coefficient.

### 2.8. Regeneration and reuse studies for biosorbent

Regeneration studies are one of the main studies which carried out as evidence for reusability of biosorbent. Desorption either thermal or non-thermal is one of methods of regeneration technique. Chemical non thermal desorption is the selected method to recycle biosorbent in this study (Alsawy et al., 2022). This method carried out in two steps, the first step is one cycle using more than one desorbing agent as (0.1 N of each HCl, NaOH, HNO$_3$, H$_2$SO$_4$ and EDTA) to select the most effective substance. The second step is to use the selected agent for five repetitive cycles. Each cycle was studied in biosorption batch system at conditions as (arsenic concentration 25 mg/l, biosorbent dose .6 g/l, contact time 1 h, and temperature 25 °C) followed by desorption experiment in which biosorbent weight was added to 100 ml of desorption agent containing medium of in 250 ml conical flask with shaking speed 300 rpm for 1 h at temperature 25 °C (Chatterjee and Abraham 2019). Desorption efficiency, removal percentage and desorption capacity calculated according to Eqs. (21), (22), and (23);

$$\text{Desorption efficiency (\%)} = (C_{de}/C_{ad})/100 \qquad (21)$$

$$\text{Removal percentage (\%)} = ((C_i - C_t)/C_i) \times 100 \qquad (22)$$

$$q_{de} = (C_{de}/M)*V \qquad (23)$$

where $C_{de}$ mg/l heavy metal desorbed, $C_{ad}$ is heavy metal absorbed mg/l, $C_i$ is initial heavy metal concentration mg/l, $C_t$ is heavy metal concen-tration at time mg/l, V is volume of eluent agent (L), M is mass of bio-sorbent (g) and $q_{de}$ is desorption capacity (mg/g).

### 2.9. Statistical analysis

All trials carried out in triplets by ICP Inductively Coupled Plasma (PerkinElmer avio 220 max USA) and average values are presented in the results and expressed as average ±SD and charts applied by Microsoft office excel and origin 2019 (Mohamad et al., 2015).

### 3. Results and discussion

#### 3.1. Optimization the biosorption efficacy of arsenic (III) by Chlamydomonas sp.

To ascertain the impact of pH on the bioremediation of As (III) by the studied microalga, a fluctuation range of pH values (pH 3.0–8.0) was used. As shown in Figure 1, the optimum pH for biosorption capacity was 4. The data recorded in Figure 1 exhibit the elimination capacity of As (III) ions increased gradually from 18.5 mg/g at pH 3–28.4 mg/g at pH 4. Through the experimental study about the influence of different pH values on the adsorption capacity of the dry biomass of *Chlamydomonas* sp. as shown in Figure 1, we found a steady increase in the adsorption operation of arsenic ions (III) reached 28.4 mg/g on the surface of *Chlamydomonas* sp. biomass by increasing the pH to 4. On this point, the
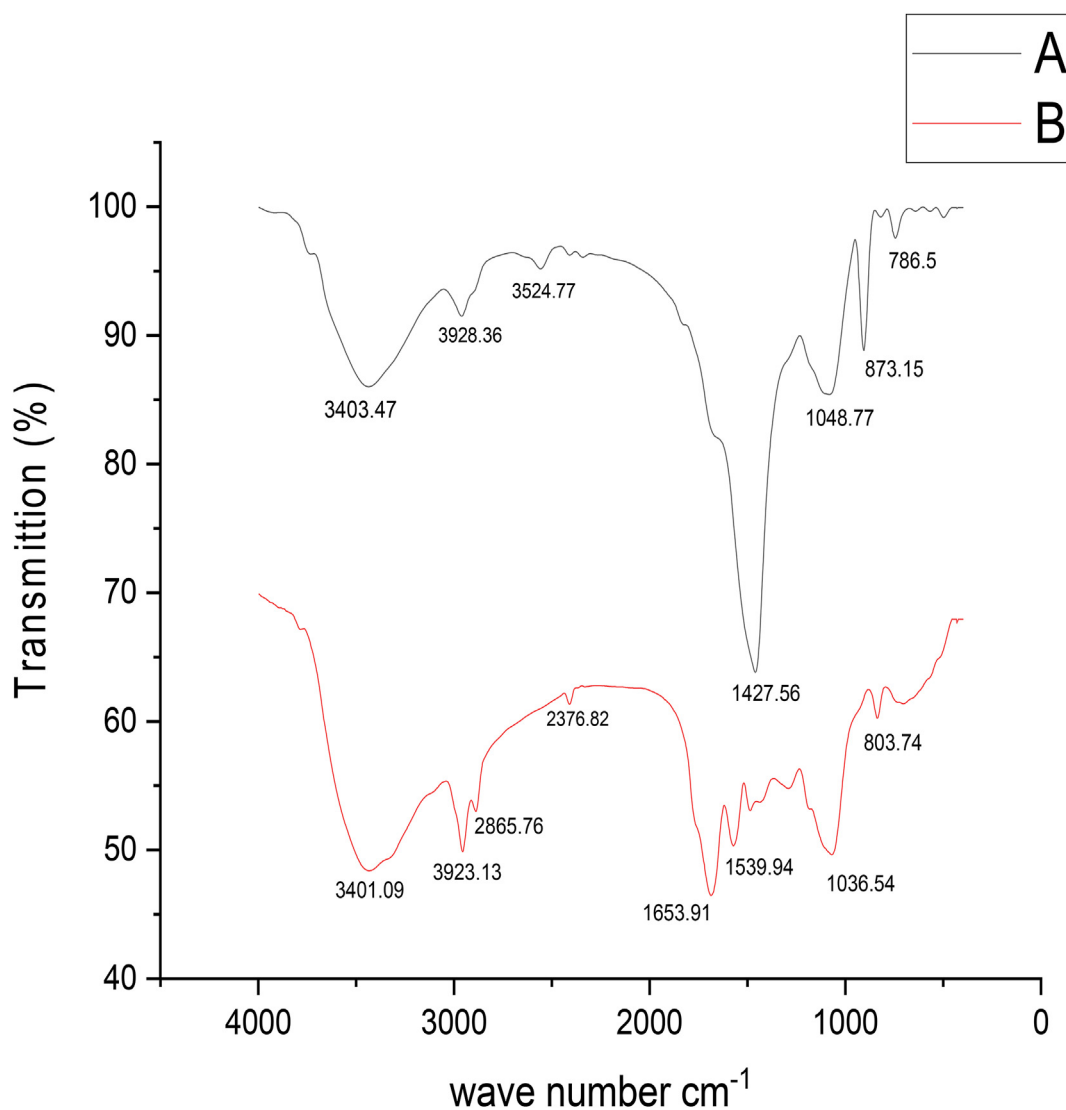
**Figure 7.** FTIR for (A) unloaded controlled biomass and with characteristic peaks weave length & for (B) As (III) loaded controlled biomass with characteristic peaks weave length.

negative charge of active sites of biosorbent was more charged. It was plant that raising rained pH is more available to the biosorption of heavy metal cations (Long1 et al., 2021). The pH of the water mixture is considered an appreciable employee for ion biosorption due to its effect on the charge of the biosorbent exterior and thus the solubility of the ions (Abdel-Raouf et al., 2022). This was in harmony with previously suggestions, which reported that a reduction in pH is accompanied by a rising in the level of metal sorption (Chu and Phang, 2019). Positively charged surface sites aren't acceptable for attraction of heavy metal cations because of electrostatic repulsion. Rising of pH followed by increasing of active sites with negative charge leading to attract more cations for binding (Khajavian et al., 2019). The data indicate that, Continuous increasing to pH 7 leads to significant decreasing in biosorption capacity due to formation of insoluble metal hydroxide. On the other hand, interference, and compensation between $OH^-$ anion and heavy metal cations causing metal precipitation according to Maisarah et al. (2021). It's an essential factor of heavy metal bioremoval.

As a result of mentioned above at low pH their abundance of $H^+$ which decrease the chance of biosorption because of competition with arsenic cation on binding active site in adsorbent, by increasing pH 4, the abundance of $H^+$ decrease leading to increasing biosorption reaching to optimum biosorption, continuous increasing pH 5, $OH^-$ ions start to be

remarkable resulting in slightly decreasing in arsenic biosorption due to forming in soluble metal hydroxide. At pH 6 the biosorption also still decreasing reaching to neutral state at pH 7, followed by slightly alkaline media at pH 8 which steady stable qt. this clarification was proven by Zeta potential analysis which verify the pH effect at pH 3 = −22 mV, pH 4 = −34.6 mV, pH 5 = −35.5 mV, pH 6 = −39.2 mV, pH 7 = −39.4 mV and pH 8 = −39.9 mV which ensures the changing of biosorption efficacy with pH. At biosorbent dose 0.6 g/l, contact time 1 h, temperature 25 °C, variable pH (3,4,5,6,7 and 8) and initial heavy metal concentration (25, 50, 100, 140, 180 and 200 mg/l) it was observed that, the effect of pH on biosorption at high initial heavy metal concentration is limited as a comparison with low concentration.

As shown in (supporting data; Figure S2) the most observed effect is on concentration 25 and 50 mg/l from concentration 100 mg/l up to 200 mg/l there is a restricted effect. The suggested explanation is due to the abundance of heavy metal ions at high concentration leads to neglect the aggregation of $H^+$ and $OH^-$ ions either in acidic or alkaline state which give chance to the residual heavy metal ions to bind to biosorbent active sites.

Different dried microalgal biomass doses (0.2, 0.4, 0.6, 0.8, 1.0 and 1.2 g/l) were used to estimate the biosorption efficacy of As (III) at the optimum pH 4 as shown in Figure 2. It has been noted that increasing the biomass dose exceeds biosorption capacity till certain dose 0.6 g/l. At this
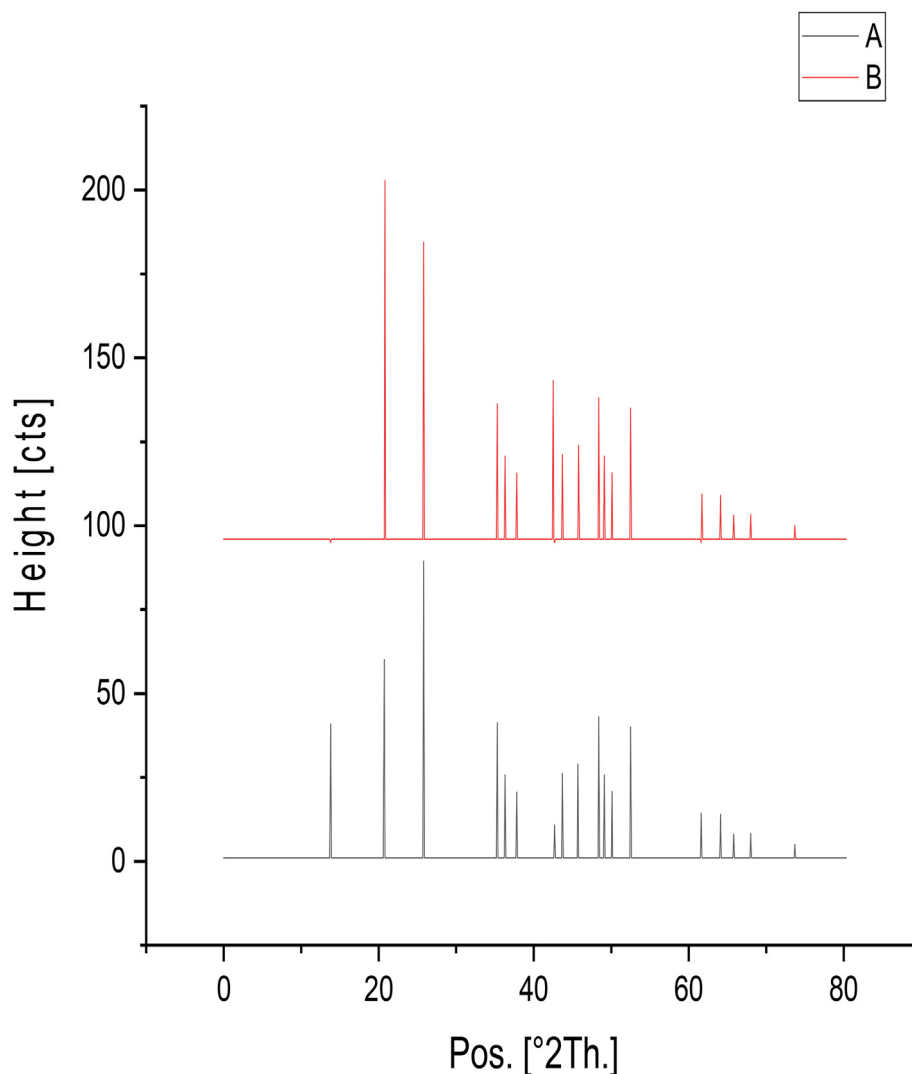
**Figure 8.** XRD for (A) unloaded controlled biomass and (B) As (III) loaded controlled biomass with characteristic peaks 2θ.

**Table 9.** XRD Peaks data features of controlled As (III) un loaded biomass and controlled As (III) loaded biomass.

| controlled As (III) un loaded biomass | | | | | |
|---|---|---|---|---|---|
| Pos. [°2Th.] | Height [cts] | d-spacing [Å] | Rel. Int. [%] | Crystallite Size only [Å] | Micro Strain only [%] |
| 20.8837 | 107.85 | 4.25374 | 62.51 | 920.3247 | 0.2311 |
| 26.6952 | 172.53 | 3.33944 | 100 | 927.0256 | 0.180116 |
| 29.6743 | 105.43 | 3.01062 | 61.11 | 643.4676 | 0.233937 |
| controlled As (III) loaded biomass | | | | | |
| Pos. [°2Th.] | Height [cts] | d-spacing [Å] | Rel. Int. [%] | Crystallite Size only [Å] | Micro Strain only [%] |
| 18.469 | 89.65 | 4.80408 | 56.93 | 48.04762 | 4.99929 |
| 21.0653 | 110.784 | 4.21748 | 83.69 | 28.93167 | 7.288699 |
| 27.9323 | 98.623 | 3.19429 | 100 | 344.279 | 0.46391 |
| 33.1376 | 20.32 | 2.70347 | 9.68 | 410.7689 | 0.329074 |

*Where (pos.) is position of peak (2Th), height is counts of peak (cts) and (Rel. int.) is relative intensity (%).

dose, the removal capacity of As (III) still attained maximum values of 49.3 mg/g. On the other hand, the As (III) removal capacity didn't show massive variance with an elevation of the biosorbent dosage.

The rate of biological absorption of the absorbent used is affected by the difference in the rate of dose used Moghadam et al. (2013). Micro-algae are well-known for their efficiency to ingest metal ions as they are necessary as vital nutrients (Gadd, 1990). In the present investigation, it was found that the increasing in biomass dose to 0.6 g/l scientifically increase biosorption capacity. This is due to increasing of active sites (Lestari et al., 2016). However, when the biomass ratio is increased, we observe a reduction in the effective adsorbent biomaterial's surface area. Thus, this can be attributed to the increased accumulation of biomass that was formed in high quantities, and this explains the rate of decrease in bio-uptake when the amount of biomass used is increased (Satya et al., 2020). It is in harmony with Finocchio et al. (2010) and Zeraatkar et al. (2016) how stated that the percentage of mineral ion getting rid of the aqueous solution is influenced by alga biomass concentration and increasing the biomass concentrations above the acceptable limit reduces the efficiency of ion uptake rate per gram of dried biomass.

To monitor effect of heavy metal initial concentration on biosorption capacity in batch system we must prepare sequences of heavy metal concentrations (25, 50, 100, 140, 180 and 200 mg/l) of arsenic at constant biomass dosage (0.6 g/l) and optimum pH (4) as shown in (supporting data, Figure S3). By increasing initial concentration, the maximum biosorption capacity increase till certain concentration (50 mg/l). At this point, the removal capacity of As (III) still attained maximum values of 60.6% followed by steady stable state. On the other
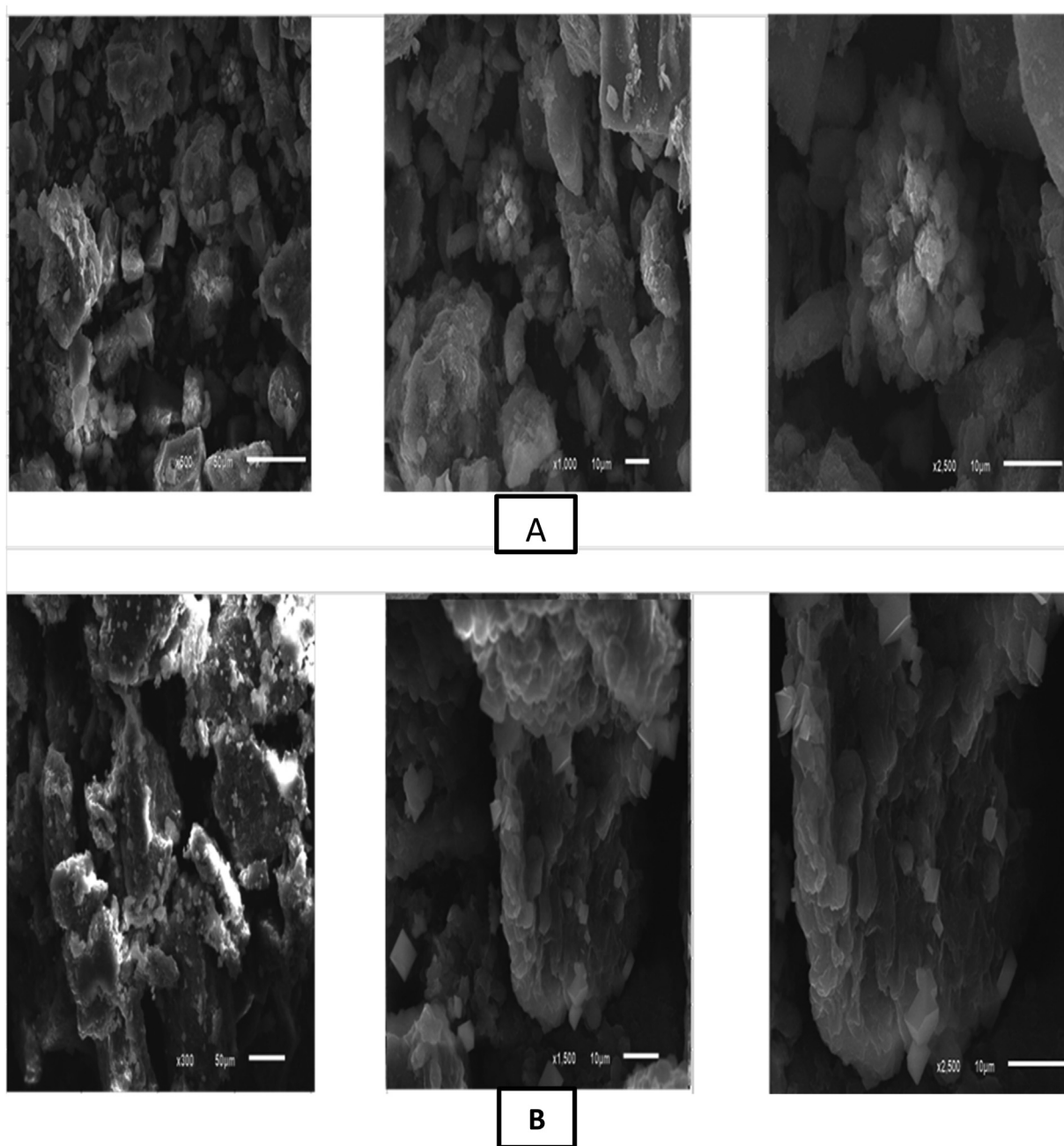
**Figure 9.** SEM of (A) controlled unloaded dried microalgae at 500, 1000 and 2500 magnification power and (B) for controlled arsenic (III) loaded biomass at 300, 1500 and 2500 magnification power.

side, at constant time removal percentage of heavy metal showed low biosorption capacity by increasing its initial concentration as shown in (supporting data, Figure S4). In addition to what was mentioned earlier the time required to gain equilibrium biosorption capacity point is directly proportional to initial heavy metal concentration as shown in (supporting data, Figure S5).

It was observed from (supporting data, Figures S3, S4, and S5) that increasing in initial heavy metal concentration leads to increase maximum biosorption capacity, decrease removal percentage and increase time required for equilibrium point. Biosorption behavior under different initial concentration of arsenic (III) ions was investigated and the data are represented in (supporting data, Figures S3 and S4). An increase in the rate of adsorption efficacy was recorded in the situation of initial concentrations of 25–50 mg/l, then there was not downward or upward trend, and the results remained stable. The highest removal

equal to 48 mg/g was achieved for the initial concentration of 50 mg/l. On the other hand, the higher used concentration of arsenic leads to a lower removal rate, which agrees with previous studies (Ali et al., 2016) which announced that the saturation of the binding sites is the influencing factor in this case. In our study, the rate of removal of arsenic ions was significantly reduced from 95.2% to 18%, and this may be for decreasing in the number of active sites available for each molecule of elemental arsenic on the surface of cells (Abdel-Aty et al., 2013).

Effect of solution temperature (15, 20, 25, 30, 35 and 40 °C) on the biosorption of As (III) ions was investigated. Figure 3 shows that when temperature was increased from 15 °C to 20 °C, the biosorption capacity of As (III) ions by dried biomass was increased from 8.5 to 22 mg/g raising of temperature from 20 °C to 25 °C make continuous raising in biosorption capacity from 22 to 49.7 mg/g still raising temperature to 30 °C and 35 °C leads to slightly stable biosorption capacity about 48.5 and
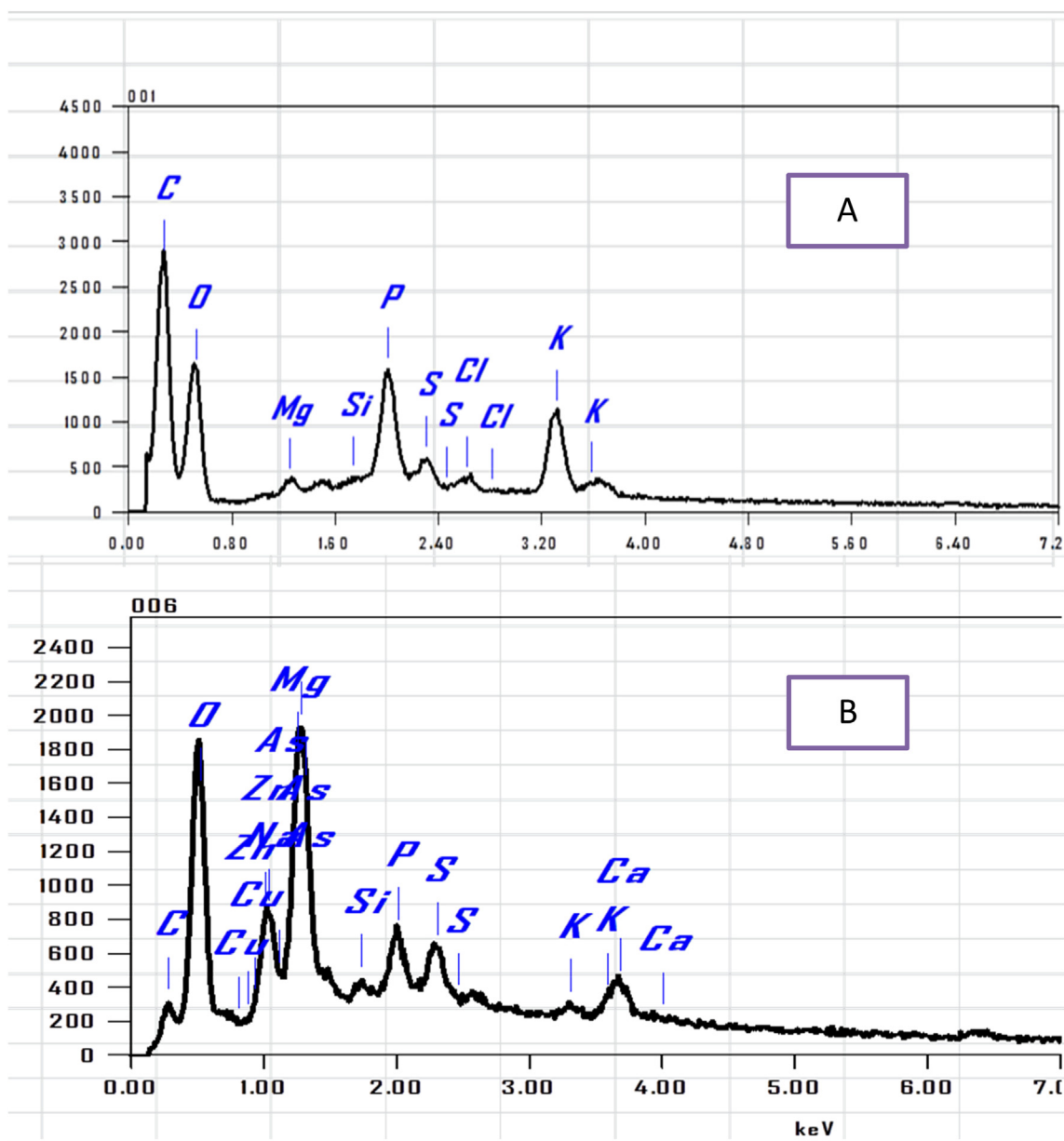
**Figure 10.** EDX peaks (A) for controlled unloaded biomass, values of peaks showing no arsenic (III) peak & (B) for controlled arsenic (III) loaded biomass, values of peaks showing arsenic (III) peak.

48 mg/g respectively. By increasing temperature to 40 °C it was observed that biosorption capacity decrease to 46.8 mg/g. From this result it is detected that viscosity in temperature leads to increasing in biosorption capacity due to decreasing liquid viscidity which leading to increase the rate of adsorbate diffusion these this conclusion is in agreement with Mohamed et al. (2014). The decreasing of biosorption capacity after temperature 35 °C is due to saturation of binding active sites on biomass add to desorption of heavy metal ions from biomass to liquid. Desorption occurs due to weakness of electrostatic interaction between heavy metals ion and active binding sites (Ali et al., 2015). From all these inferences, the optimum biosorption temperature is 25 °C.

The result of the exposure period on the biosorption rate was shown in Figure 4. The data exhibited the biosorption of As (III) ions was fastest in the initial 30 min, then increased gradually till equilibrium was accomplished at 60 min (removal capacity of As (III) 50 mg/l). Next to this stage, the biosorption became nearly stable. Consequently, the

uptake ($q_e$) of As (III) and adsorbed As (III) concentrations ($C_e$) at the end of 60 min are given as the optimal values (known as equilibrium point), and did not show any significant alterations through the contact time. Measuring of biosorption capacity at several times during process at constant biomass and constant optimum pH as shown in Table 1 and Figure 4 Regarding the effect of handling time on the efficiency of the alga used in its ability to remove arsenic toxicity, the results showed that the algae's efficiency in removing arsenic (III) ions was steadily increase from the beginning of the experiment until equilibrium was achieved after 1 h. This may be due to the available active site's number on the surface of algal cells (Malkoc and Nuhoglu, 2003; Abdolali et al., 2016). However, the decrease in the removal rate in the following stages, it may be as a reason of the diffusion of metal ions and competition among them for all the binding sites on the surface of the cell of the used alga (Vogel et al., 2010; Bishnoi et al., 2007), which leads to an increase in the time to reach to the equilibrium point.

**Table 10.** EDX for controlled unloaded biomass, values of peaks showing no arsenic (III) peak for controlled arsenic (III) loaded biomass, values of peaks showing arsenic (III) peak.

| unloaded biomass | | | | |
|---|---|---|---|---|
| Element | (KeV) | Mass% | Error% | Atom% |
| C K | 0.277 | 53.25 | 0.16 | 62.31 |
| O K | 0.525 | 39.24 | 0.67 | 34.47 |
| Mg K | 1.253 | 0.6 | 0.15 | 0.35 |
| Si K | 1.739 | 0.16 | 0.1 | 0.08 |
| P K | 2.013 | 3.08 | 0.08 | 1.4 |
| S K | 2.307 | 0.78 | 0.07 | 0.34 |
| Cl K | 2.621 | 0.34 | 0.08 | 0.13 |
| K K | 3.312 | 2.56 | 0.09 | 0.92 |
| Total | | 100 | | |
| arsenic (III) loaded biomass | | | | |
| Element | (KeV) | Mass% | Error% | Atom% |
| C K | 0.277 | 27.27 | 0.45 | 40.46 |
| O K | 0.525 | 46.93 | 0.47 | 45.57 |
| Mg K | 1.253 | 5.44 | 0.18 | 3.99 |
| As K | 1.282 | 12.03 | 0.37 | 3.34 |
| Si K | 1.739 | 3.62 | 0.18 | 0.39 |
| P K | 2.013 | 2.32 | 0.14 | 1.33 |
| S K | 2.307 | 2.48 | 0.1 | 0.82 |
| Total | | 100 | | |

### 3.2. Biosorption kinetics

The kinetic models have the potential to discover effective procedures and phases in the adsorption process. First order, second order and elovich are the most common models illustrating adsorption kinetics process. first order suggests that rate of action is directly proportional to adsorbate concentration, second order demonstrate that rate of action depends on adsorption capacity not on adsorbate concentration, one of most benefits of second order is the ability to calculate equilibrium adsorption theoretically instead of evaluating it empirically (Foroutan et al., 2021d). Elovich kinetic model assumes that the rate of adsorption of solutes decrease exponentially as the amount of adsorbed solute increase. Charts of kinetic models for biosorption of As (III) at different initial concentration as shown in (supporting data, Figure S6:11) and values for these chart represented in attached table file as shown in (supporting data, Table S1:12). Tables show slope, $q_{max}$, $R^2$ and kintec constant values for 1st order, 2nd order and elovich models for biosorption kinetics of As (III) at different initial concentration as shown in Tables 2, 3, and 4. It appears from previous calculations that nearest theoretically calculated $q_{max}$ to measured one (Savari et al., 2020) in addition to the regression correlation coefficients $R^2$ gives higher value which suggest the preferred kinetic model occurs in biosorption mechanism for each initial heavy metal concentration (Ali et al., 2016). According to this fact the suggested kinetic model for initial heavy metal concentration 25 mg/l is 2nd order, for 50 mg/l is 1st order, for 100 mg/l is elovich, for 140 mg/l is elovich, for 180 mg/l is 1st order and for 200 mg/l is elovich. In addition to mentioned three models the Intraparticle

## Results

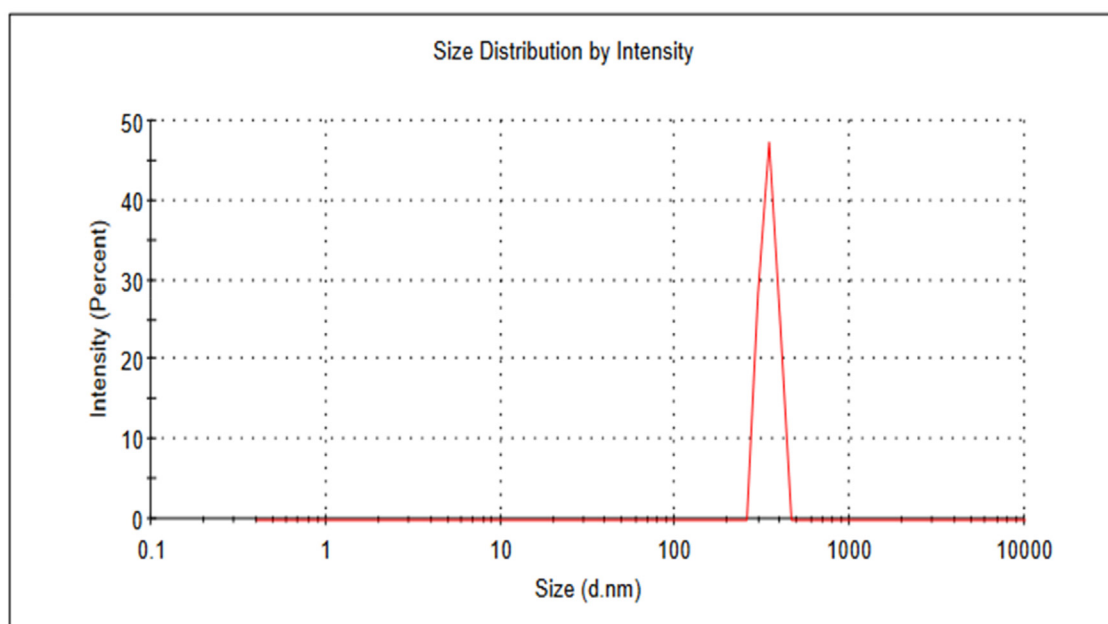|  | | Size (d.nm... | % Intensity: | St Dev (d.n... |
|---|---|---|---|---|
| Z-Average (d.nm): 1174 | Peak 1: | 342.0 | 100.0 | 36.45 |
| Pdl: 1.000 | Peak 2: | 0.000 | 0.0 | 0.000 |
| Intercept: 1.07 | Peak 3: | 0.000 | 0.0 | 0.000 |
| Result quality | Refer to quality report | | | |



**Figure 11.** DLS chart for dried *Chlamydomonas* sp. biomass showing average particle size 1174 nm and PDI = 1.
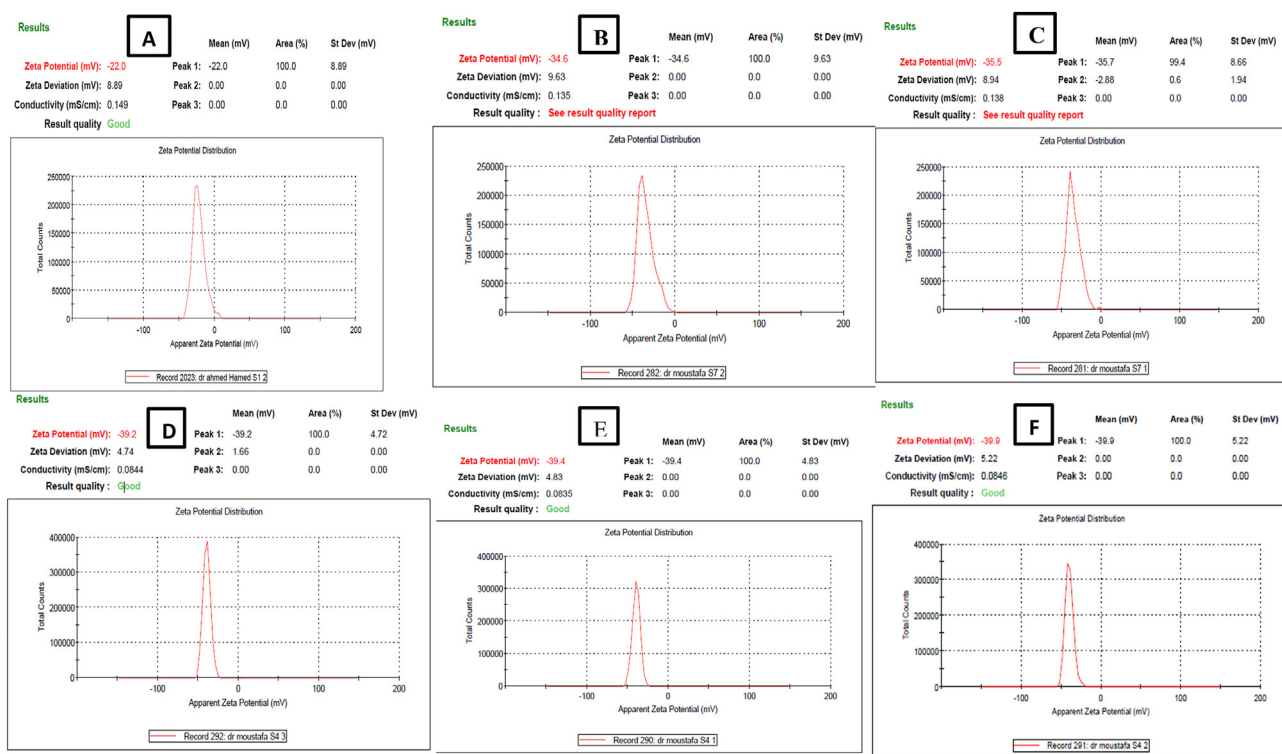
**Figure 12.** Zeta potential chart for (A) dried *Chlamydomonas* sp. biomass at pH 3, recorded -22 mV potential and 0.149 mS/cm conductivity. (B) for dried *Chlamydomonas* sp. biomass at pH 4, recorded -34.6 mV potential and 0.135 mS/cm conductivity. (C) for dried *Chlamydomonas* sp. biomass at pH 5, recorded -35.5 mV potential and 0.138 mS/cm conductivity. (D) for dried *Chlamydomonas* sp. biomass at pH 6, recorded -39.2 mV potential and 0.0834 mS/cm conductivity.(E) for dried *Chlamydomonas* sp. biomass at pH 7, recorded -39.4 mV potential and 0.0835 mS/cm conductivity. (F) for dried *Chlamydomonas* sp. biomass at pH 8, recorded -39.9 mV potential and 0.0846 mS/cm conductivity.

diffusion model, as shown in (supporting data Figure S12) that the graph between $q_t$ and $t^{0.5}$ wasn't linear which resemble that the intraparticle diffusion was not the rate controlling step in these adsorption systems (Lim et al., 2008). The graph consists of three regions the fist ne indicate to fast absorption of arsenic followed by the second region in which the adsorption is slow due to ions have to penetrate the intraparticle pores to adsorb onto the pore surface area of the particles and thus the intraparticle diffusion become rate limiting step. The last region marked the slope is near to zero showing that tha active binding sites on adsorbent become saturated and reached to equilibrium state (Sreedhar and Reddy 2019). From date reported in Table 5 it can be detected the greater intercept C is the greater effect of boundary layer diffusion.

### 3.3. Biosorption isotherm

Interaction in adsorption occurs in 5 types of process: between adsorbate-adsorbate adsorbent-adsorbate, adsorbent-solvent, adsorbate-solvent, and solvent-solvent. In order the adsorption process to occur, the adsorbent-adsorbate interaction should be the strongest one (Patiha et al., 2016). From the relative research of the direct charting of Langmuir, Freundlich, Temkin and Dubinin-Radushkevich models, it was obtained that the $R^2$ value is 0.995 of Langmuir isotherm model for As (III) while its 0.982 for Freundlich isotherm, 0.9381 for Temkin and 0.9655 for Dubinin – Radushkevich as shown in Tables 6 and 7 and Figure 5. Values of $R^2$ indicate that the metal ion removal mechanism is observed to appropriate well with the Langmuir isotherm model and this also propose that the biosorption has nonstop biosorption energy in Langmuir model. The monolayer is formed if the strength of the bond between adsorbate-adsorbent molecules is stronger than other 4 interaction. The binding site of the first adsorbed molecules will act as the initiator to the site of the next adsorbed molecule. The second molecule will be binded strongly to the first molecule, and because of strong

adsorbent-adsorbate interaction, besides and not above (Foroutan et al., 2020). In other words, the Langmuir isotherm goes well with resulted data substantially cue to the homogeneous expansion of active binding sites on the face of dried biomass. As the face is homogeneous the maximum biosorption capacity was planted to be 52.9 mg/g for As (III) (Obulapuram et al., 2021).

### 3.4. Biosorption thermodynamic

The bioremoval efficacy of heavy metal by dried microalgae was examined under variable temperature within range (15, 20, 25, 30, 35 and 40 °C). From resulted data it was observed that bioremoval mechanism is dependent on temperature as shown in Figure 3. The optimum temperature for bioremoval mechanism is 25 °C (Yogeshwaran and Priya 2022). Data resulted from plotting 1/T versus lnk in Figure 6 Were reported in Table 8. The negative free energies calculated in this study were −0.2412 kJ/mol, −0.7304 kJ/mol, −2.2289 kJ/mol, −2.1805 kJ/mol, −2.18 kJ/mol and −2.1308 kJ/mol respectively at temperature 288, 293, 298, 303, 308 and 313 K verify that the nature of the process is spontaneous nature. The endothermic nature of process is deduced through positive value of ΔH (+22.65 kJ/mol). The entropy ΔS was calculated (+80.75 J/mol K) which characterize the randomness of process. This value shows that there is attraction of heavy metal ions As (III) towards algal bioadsorbents (Kumar et al., 2020).

### 3.5. Effect of inorganic ions

The bioremediation may be limited due to presence of inorganic ions which can covert the sorbent–sorbate interaction. When the effect of these ions is well known, Thus, the effect of $Na^+$, $K^+$ and $Ca^{2+}$ ions on the biosorption of As (III) was investigated. The resulted data was plotted in (supporting data, Figure S13). From this figure it's observed that
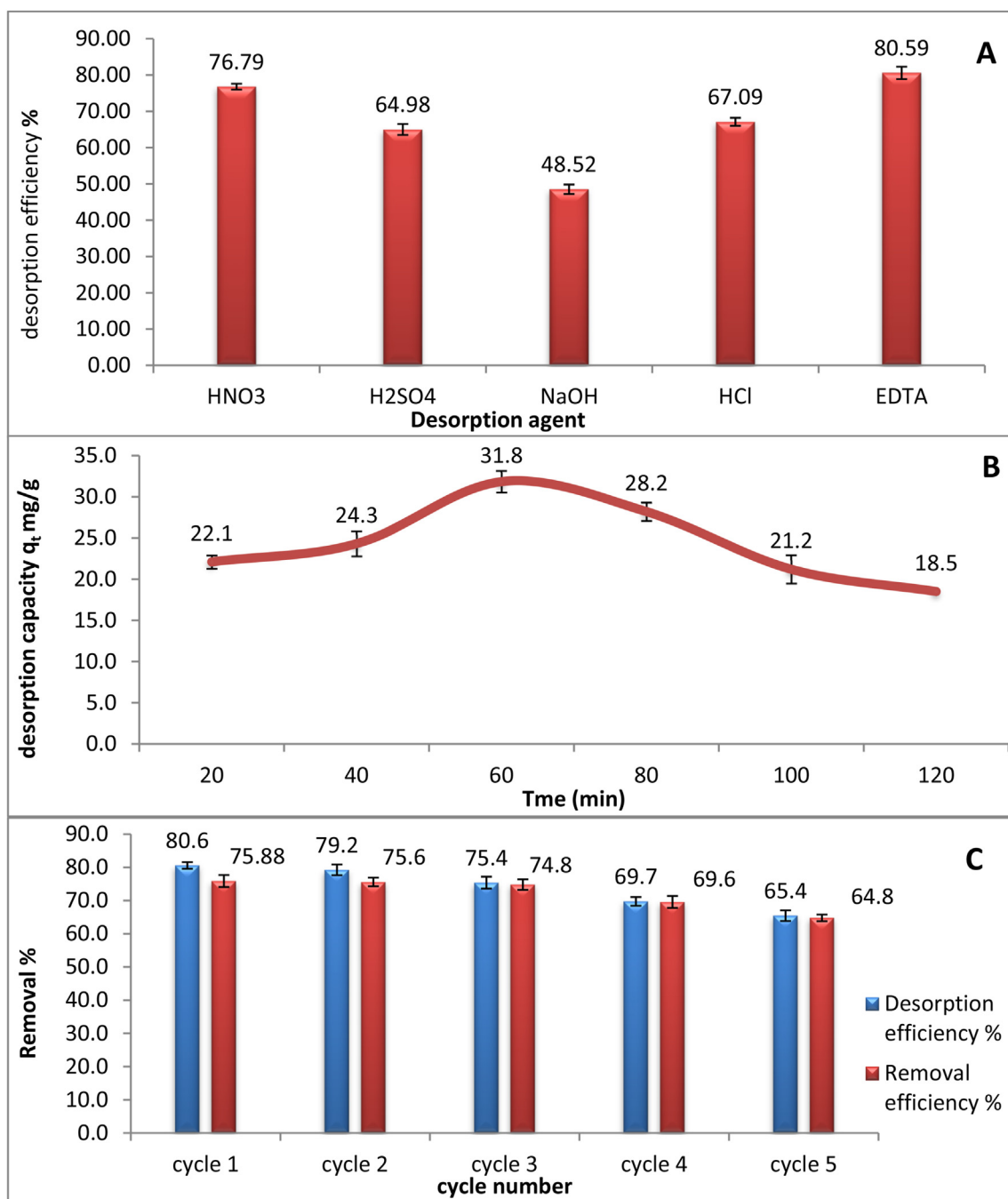
**Figure 13.** (A) represents comparison among different eluent agent as (HNO₃, H₂SO₄, NaOH, HCl and EDTA) in desorption efficiency %. (B) represents the change of desorption capacity (mg/g) with time (min) using EDTA as eluent agent. (C) represents 5 regeneration cycles using EDTA as eluent agent. All experiments were carried out at arsenic (III) concentration 25 mg/l, biomass dose 0.6 g/l, temperature 25 °C, pH 4 and contact time 1 h.

monovalent ions have a slight influence in biosorption process. On the other hand, the divalent ion has more potential effect. The strength of inhibition by the inorganic ions expressed as the sequence: $Ca^{+2} > K^+ > Na^+$ for arsenic (III). By the way, the effects of inorganic ions ($Na^+$, $K^+$, and $Ca^{2+}$) may act as a competition for biosorption sites with As (III) ions as a reason of binding to active sites of biosorbent; reduction in the activities of metal, thus limiting their transporting to the surface of dried biomass; and improve aggregation of in organic ions in the surface of biosorbent by electrolyte ions through electric double layer compression. So, $Na^+$, $K^+$ and $Ca^{2+}$ inhibited the biosorption of As (III) with raising ion concentrations. The monovalent cations $Na^+$ and $K^+$ did not much affect the biosorption even at high concentrations. The effects of $Ca^{2+}$ are more

effective than $K^+$ and $Na^+$ because of their stronger affinity with OH groups (Tounsadi et al., 2015).

### 3.6. Biomass characterization

To identify the functional groups within dry biomass of *Chlamydomonas* used in the our study case, an experiment was conducted to determine the spectrum curves using FTIR, where it was found that they were confined between 400 and 4000 cm⁻¹ before and after the biosorption experiment as shown in Figure 7 and (supporting data, Figure S14). The spectra of FTIR for dried microalgae before arsenic (III) biosorption process show significant peaks at 3403.74, 2928.36,

**Table 11.** Comparison between *Chlamydomonas* sp. as biosorbent in this study and other biosorbent in previous studies for arsenic (III).

| Adsorbent | Conditions | Adsorption capacity (mg/g) | Removal efficiency % | Reference |
|---|---|---|---|---|
| *Scenedesmus*. sp. | Dose: 0.8 g/l<br>Concentration: 30 mg/l pH: 4.0<br>Temperature: 32 °C | 23 mg/g | 97.89% | (El-Naggar et al. 2020) |
| *Chlorella vulgaris* | Contact time: 210 min<br>Dose: 6 g/l<br>Concentration: 25 mg/L pH: 6.0<br>Temperature: 50 °C | 13 mg/g | 95% | (Ghayedi et al., 2019) |
| *Scenedesmus obliquus* | Contact time: 180 min<br>Dose: 0.8 g/l<br>Concentration: 400 ppb pH: 7.0<br>Temperature: 29 °C | – | 72% | (Mohkami and Pirkoohi, 2019) |
| *Scenedesmus sp.* | Contact time: 36 h.<br>Dose: 0.8 g/l<br>Concentration: 30 mg/L pH: 4.0<br>Temperature: 32 °C | 28 mg/g | – | (Sibi, 2014). |
| nanoscale zero-valent iron stabilized with starch and carboxymethyl cellulose | Contact time: 5 min.<br>Dose: 0.3 g/l<br>Concentration: 1 mg/l pH: 5.0<br>Temperature: 25 °C | 12.2 mg/g | 77.26% | (Mosaferi et al., 2014) |
| chitosan-coated biosorbent | Contact time: 24 h.<br>Dose: 0.2 g/l<br>Concentration: 100 ppm pH: 4.0<br>Temperature: 25 °C | 56,5 mg/g | – | (Veera et al., 2008) |
| Goethite | Contact time: 24 h.<br>Surface area: 12.7 m$^2$/g<br>Concentration: 1000 mg/l pH: 5.5<br>Temperature: 25 °C | 7.5 mg/g | – | (Ladeira and Ciminelli, 2004) |
| *Chlamydomonas* sp. | Contact time: 60 min<br>Dose: 0.6 g/l<br>Concentration: 25–200 mg/L pH: 4.0<br>Temperature: 25 °C | 53.8 mg/g | 95.2% | This study |

2524.77, 2375.86, 2308.75, 1427.56, 1048.77, 873.15, 786.50, 711.69, 608.66, 534.60 and 464.75 cm$^{-1}$ and after biosorption process of arsenic these peaks shifted to 3401.09, 2923.13, 2855.76, 2376.82, 1653.91, 1539.94, 1453.93, 1258.11, 1036.45, 803.74 and 670.82 cm$^{-1}$. The data in Figure 7 demonstrate that there is observed broading and merging in characteristic peaks. The Peaks around 3400 cm$^{-1}$ were distinctive the –NH and –OH groups. The Peaks ranged approximately at 2900 cm$^{-1}$ were from the C–H expansion way. The peaks at 1640 cm$^{-1}$ and 1636 cm$^{-1}$ indicated the presence of carboxylic C=O expansion (COOH). The peaks at 1427 cm$^{-1}$ and 1453 cm$^{-1}$ approved the existence of an amide group. The peaks at 1258 cm$^{-1}$ exhibited the presence of P=O and C–N expansion manner. The peaks at 1048 cm$^{-1}$ and 1036 cm$^{-1}$ represent asymmetric stretching modes of Si–O bond, and in total peaks at 464, 534, 803 and 670 cm$^{-1}$ refer to metal compounds. Regarding the FTIR analysis, various types of vibrational frequencies because of several function groups were detected in FTIR spectrum of the microalgal biomass. Abroad band at 3403.47 cm$^{-1}$ in adsorbent is indicator of the occurrence of free and hydrogen bonded OH groups on biosorbent (Gaur et al., 2018). While the band at 1427 cm$^{-1}$ representing stretching amide (C–N and N–H) of proteins. Also, the peaks located at 1637–1617 cm$^{-1}$ are representing carbonyl group (–HC = O, R2 C=O) stretching. Representing Aliphatic C–H group appears by the bands at 2928.36 cm$^{-1}$. The bands to the S–H stretching group 2375 cm$^{-1}$ S–H stretching group for *Chlamydomonas* band 1427 cm$^{-1}$ resembles to the free C=O asymmetric stretching modes of Si–O–Si bonds represented at 464.65 and 1048.77 cm$^{-1}$ correspond. Also the bands at 466 cm$^{-1}$ represent metal compounds (Kamble et al., 2018) stated that the main components the microalgae are proteins, lipids, and polysaccharides, which provide active variable functional groups. The main differences between the experimented biomass within range approximately 1000–1600 cm$^{-1}$. FTIR spectra of the native and loaded with As (III) prove that the cations of heavy metal can be attached to the hydroxyl, carboxyl, and amino groups found on algal biomass so that an indictable brooding in O–H

bonds at 3400 cm$^{-1}$ is strong evidence for heavy metal biosorption in agreement with Godlewska et al. (2018).

X-ray diffraction is a non-damaging method used to explain details for data on the crystal features arrangement of materials. This technique offers many benefits e.g. high accuracy, Non-damaging, and able to investigate polycrystalline, single crystals, or amorphous substance. XRD has been generally involved in explanation of biosorbent and in the confirmation of heavy metals biosorption process. By using origin 2018 software which enables us to make a comparison among peaks of biosorbent *Chlamydomonas* loaded and un-loaded with As (III) as shown in Figure 8 which observed in As-loaded biomass through newly formed peak at 2θ 18.469 and shifting of peaks at 2θ 20.8837 and 26.6952 to 2θ 21.0653 and 27.9323 respectively. It's confirmed by reported chart of loaded and unloaded biomass as shown in (supporting data, Figure S15) and Table 9. Resulted patterns of X-ray diffraction of biomass. Prior and post As (III) biosorption process. Peaks with Sharp intensity in the unloaded biosorbent has been found at 2θ = 20.8837, 26.6952 and 29.6743, with d spacing value of 4.25374, 3.33944 and 3.01062. Otherwise the pattern in the As-bound biosorbent showed the appearance of new peaks at 2θ values about 13.8043 for As (III) indicating for character of the biosorbent. The XRD data analysis of the unloaded biosorbent illustrates common diffraction peaks.

Sharp peaks were observed associated with crystalline shape (Al Moharb et al., 2020). This indicates crystallinity of pure *Chlamydomonas* biomass. Further, observation of changing in 2θ and d-spacing values As (III)-loaded biomass verifies that there was a change in crystallinity of biosorbent (Sarada et al., 2017). In the spectra the biosorbent revealed reported peaks, which propose that these metal ions can efficiently biosorbed into the biomass. These results are harmony with Kanamarlapudi and Muddada (2019) who stated that, the amorphous character of biosorbent in the spectra is marked by the poorly persistent peaks, which propose that the metal ion can clearly permeate into the surface, which is profitable for metal biosorption from aqueous solutions.

As mentioned previously SEM technique detect biosorption process through performance morphological features of dried microalgae before and after biosorption process. SEM allows observing any mechanism in which biosorption occurred. As shown in the untreated *Chlamydomonas* sp. biomass and the treated biomass as shown in Figure 9, we found the whole cell size increased in the treated biomass as compared to the untreated one's blank cells. The dried microalgal biomass pre and post bioremediation process was examined under SEM as shown in Figure 9. The SEM mechanism is simple method to detect the change in morphology of dried biomass comparing the state pre and post bio-removal process.

Crystal form of removed heavy metal proves a reduction mechanism. Tiny plaque-type solid crystals were distributed and embedded on the surface of biomass EDX emphasizes on the crystals affirm that this phenomenon is caused by biosorption of As (III) in a solid-state (Jin et al., 2016). It may be associated with other biosorption mechanisms as ion exchange and coordination (Seo et al., 2013).

The EDX spectra of biomass sample are shown in Figure 10. It is noteworthy that EDX analysis enables to provide information about the composition of the biomass surface, comparison of peaks pre and post biosorption it observed arsenic peak at 1.282 keV, as shown in Table 10. In the present investigation, it was exhibited that, the microalga biomass is distinguished by perfect biosorption efficacy and can actively bind to its surface.

The EDX mapping obviously showed that arsenic was uniformly dispersed over the surface of the investigated dry microalgal biomass. Using EDX manner it was also exhibited that the tested ions were successfully engaged to the surface of the studied microalga biomass. EDX technique is applied to identify of binding sites of arsenic ion was observed which was replaced throughout the biosorption process with absorbent ions this second biosorption mechanism occurs add on reduction as mentioned previously. The change in the intensity of peaks signals of these ions obtained by reducing or disappearing (El Sheekh et al., 2019).

On the other hand, the obtained DLS data indicated that there is particle size uniformity which plays a significant role in heavy metal bioremoval pathway rate (Piasecka et al., 2019; Castro et al., 2021) like other techniques which used to measure particle size (DLS) estimation of dry mass. The dynamic light scattering (DLS) method was used for confirming uniformity and single phasing biomass particles. Average particle size of dried biomass is 342 nm as shown in Figure 11.

Measuring of zeta potential results eventuality values of the biosorbent at the adsorption at different pH were listed the attained results exhibit that advanced mean of zeta potential values affected by pH with clearly positive effect on sorption capacity. From above values of ZP for dried biomass at pH (3, 4, 5, 6, 7 and 8) it is observed that zeta potential increase by increasing pH confirm that the charge in biomass surface change by different pH. Hence –ve charge in pH 3 = −22 mV, pH 4 = −34.6 mV, pH 5 = −35.5 mV, pH 6 = −39.2 mV, pH 7 = -−39.4 mV and pH 8 = −39.9 mV as shown in Figure 12. Collected measured information of ZP on the steadiness and charge behavior through detecting the potential of the shear plane of substance particle occurs when it moves in liquid (Savvidou et al., 2021). These data ensure that the biosorbent at pH 4 is the optimum point due to it has maximum –ve charged active site increasing biosorption capacity proven the previous results in pH optimization section. As a result of all of this, changing of –ve charge value from pH 3 to pH 4 prove that optimum biosorption occurred for positively charged heavy metal ions in pH 4 as shown in (supporting data, Figure S16). From mentioned apparatus used for biosorbent characterization, the suggested adsorption mechanism is ion exchange add to reduction process.

### 3.7. Regeneration and reuse

As result of detecting the reusability of dried microalgae as biosorbent, the first step was the selectivity of the best eluent agent. The results of desorption efficiency according to these results ($HNO_3$:76.79%, $H_2SO_4$: 64.98%, HCl: 67.09%) show that acids are the best agents as shown in Figure 13A because of abundance of protons (Bayuo et al., 2020). By contrast the least eluent efficiency was 0.1 NaOH with desorption efficacy 46.84%. EDTA shows the most effective desorbing agent about 80.59% due to its chelating properties. Another experiment was carried out to detect the optimum contact time for desorption process which explain that 60 min was the compliance contact time as shown in Figure 13B. The final experiment was five cycles running for the same eluent agent (Kumar et al., 2020). Each cycle is desorption/adsorption mechanism, as a result of these desorption efficacy tests, after the 5th cycle was 65.4% and for biosorption efficiency was 64.8% as shown in Figure 13C. Proving that *Chlamydomonas* sp. is an effective reusable dried biosorbent.

### 3.8. Comparison between dried Chlamydomonas sp. with other adsorbents in removal of arsenic (III)

Table 11 compares the maximum adsorption capacity $q_m$, and arsenic (III) removal percent of variable adsorbents tested in the literature with dried *Chlamydomonas* sp. It illustrate that $q_m$ values for various adsorbents vary significantly (Mosaferi et al., 2014; Ghayedi et al., 2019; Sibi, 2014; Veera et al., 2008). These reported results. In comparison to other adsorbents, showed that dried *Chlamydomonas* sp. had potential adsorption efficiency for arsenic (III) from aqueous solutions.

## 4. Conclusions

The data in this study indicated that, *Chlamydomonas* sp. can be applied as a biosorbent for the removal of As (III) ions from aqueous solution which is potentially affected by parameters as pH, contact time, biosorbent dose, temperature and initial metal ion concentration. The studied in these exploration colorful styles of removing heavy metal are delved and the birth approach is stressed medium of this mechanism. Likely it was used as a powerful biosorbent material (0.6 g/l concentration) for removal of As (III) from aqueous solution up to 200 mg/l at temperature 25 °C and pH 4. Isotherm Kinetic models and thermodynamics were successfully used for mathematical purposes of biosorption of arsenic ion (III) to dried biomass. Characterizations of biomass using FTIR, XRD, SEM-EDX, TEM, DLS and zeta potential prove that biosorption process occurred. Finally, it was conscripted that *Chlamydomonas* sp. is effective, reusable, low cost and environmentally friendly as a biosorbent factor for As (III) ions bioremoval from aqueous solution.

## Declarations

### Author contribution statement

Ibraheem B.M. Ibraheem; Walaa G. Hozayen; Reem Mohammed Alharbi; Mostafa S. Mohamed: Conceived and designed the experiments; Performed the experiments; Analyzed and interpreted the data; Wrote the paper.

### Data availability statement

Data will be made available on request.

### Declaration of interest's statement

The authors declare no competing interests.

## Additional information

## Acknowledgements

## References

Abdel-Aty, A.M., Ammar, N.S., Abdel Ghafar, H.H., Ali, R.K., 2013. Biosorption of cadmium and lead from aqueous solution by fresh water alga *Anabaena sphaerica* biomass. J. Adv. Res. 4 (4), 367–374.

Abdel-Rahman, G., 2022. Heavy metals, definition, sources of food contamination, incidence, impacts and remediation A literature review with recent updates. Egypt. J. Chem. 65, 419–437.

Abdel-Raouf, N., Sholkamy, E.N., Bukhari, N., Al-Enazi, N.M., Alsamhary, K.I., Al-Khiat, S.H., Ibraheem, I.B.M., 2022. Bioremoval capacity of Co$^{+2}$ using *Phormidium tenue* and *Chlorella vulgaris* as biosorbents. Environ. Res. 204, 25583–25591.

Abdolali, A., Ngo, H.H., Guo, W., Lu, S., Chen, S.-S., Nguyen, N.C., 2016. A breakthrough biosorbent in removing heavy metals: equilibrium, kinetic, thermodynamic and mechanism analyses in a lab-scale study. Sci. Total Environ. 542, 603–611.

Al-Homaidan, A.A., Al-Qahtani, H.S., Al-Ghanayem, A.A., Ameen, F., Ibraheem, I.B.M., 2018. Potential use of green algae as a biosorbent for hexavalent chromium removal from aqueous solutions. Saudi J. Biol. Sci. 25, 1733–1738.

Ali, A.A.-H., Jamila, A.A., Amal, A.A.-H., Abdullah, A.A.-G., Aljawharah, F.A., 2015. Adsorptive removal of cadmium ions by *Spirulina platensis* dry biomass. Saudi J. Biol. Sci. 795–800.

Ali, H., Khan, E., Ilahi, I., 2019. Environmental chemistry and ecotoxicology of hazardous heavy metals: environmental persistence, toxicity, and bioaccumulation. J. Chem. 1–14.

Ali, M.H.H., Hussian, A.M., Abdel-Satar, A.M., Goher, M., Napiórkowska-Krzebietke, A., Abdels, A.M., 2016. The isotherm and kinetic studies of the biosorption of heavy metals by non-living cells of Chlorella vulgaris. J. Elementol. 21 (4), 1263–1276.

Al Moharb, S.S., Devi, M.G., Sangeetha, B.M., Jahan, S., 2020. Studies on the removal of copper ions from industrial effluent by *Azadirachta indica* powder. Appl. Water Sci. 10–23.

Alpat, Ş., Alpat1, S.K., Çadirci2, B.H., Özbayrak, Ö., 2010. Effects of biosorption parameter: kinetics, isotherm and thermodynamics for Ni(II) biosorption from aqueous solution by *Circinella* sp. Electron. J. Biotechnol. 13 (5), 1–20.

Alsawy, T., Rashad, E., El-Qelish, M., Mohammed, R., 2022. A comprehensive review on the chemical regeneration of biochar adsorbent for sustainable wastewater treatment. npj Clean Water 1–21.

Ayangbenro, A.S., Babalola, O.O., 2017. A new strategy for heavy metal polluted environments: a review of microbial biosorbents. Int. J. Environ. Res. Publ. Health 14, 1–16.

Bayuo, J., Abukari, M.A., Pelig-Ba, K.B., 2020. Desorption of chromium (VI) and lead (II) ions and regeneration of the exhausted adsorbent. Appl. Water Sci. 1–6.

Bishnoi, N.R., et al., 2007. Biosorption of Cr (III) from aqueous solution using algal biomass *Spirogyra* spp. J. Hazard Mater. 145, 142–147.

Boddu, V.M., Abburi, K., Talbott, J.L., Smith, E.D., Haasch, R., 2008. Removal of arsenic (III) and arsenic (V) from aqueous. sciencedirect 10, 633–642.

Castro, K.A., Chao, T.C., Vinet, B.D., Cisternas, C., Ciudad, G., Rubilar, O., 2021. Green synthesis of copper oxide nanoparticles using protein fractions from an aqueous extract of Brown algae *Macrocystis pyrifera*. Processes 9, 1–10.

Cavalca, L., Corsini, A., Zaccheo, P., Andreoni, V., Muyzer, G., 2013. Microbial Transformation of arsenic ; Perspectives for biological removal of arsenic from water. Future Microbiol. 8, 753–768.

Chatterjee, A., Abraham, J., 2019. Desorption of heavy metals from metal loaded sorbents and e-wastes: a review. Biotechnol. Lett. 1–15.

Chu, W.-L., Phang, S.-M., 2019. Biosorption of heavy metals and dyes from industrial effluents by microalgae. In: Microalgae Biotechnology for Development of Biofuel and Wastewater Treatment. Springer, pp. 599–634.

Dada, A.O., Olalekan, A.P., Olatunya, A.M., DADA, O., 2012. Langmuir, freundlich, Temkin and Dubinin–Radushkevich isotherms studies of equilibrium sorption of Zn$^{2+}$ unto phosphoric acid modified Rice husk. J. Appl. Chem. 3 (1), 38–45.

Dulla, J.B., Tamana, M.R., Boddu, S., Pulipati, K., Srirama, K., 2020. Biosorption of copper (II) onto spent biomass of *Gelidiella acerosa* (brown marine algae): optimization and kinetic studies. Appl. Water Sci. 10, 1–10.

El-Awamri, A.A., Abd El Fatah, H.M., Badr, S.A., Ashmawy, A.A., El-Sherif, I.Y., Moghazy, R.M., 2015. Comparative study on biosorption and desorption of three selected toxic heavy metals by some microalgae. Egypt. J. Phycol. 16, 24–46.

El-Naggar, N.E., Hussein, M.H., Shaaban-Dessuuki, S.A., Dalal, S.R., 2020. Production, extraction and characterization of *Chlorella vulgaris* soluble polysaccharides and their applications in AgNPs biosynthesis and biostimulation of plant growth. Sci Rep 10, 3011.

El-Sheekh, M., El Sabagh, S., Abou El-Souod, G., Elbeltagy, A., 2019. Biosorption of cadmium from aqueous solution by free and immobilized dry biomass of *Chlorella vulgaris*. Int. J. Environ. Res. 13, 511–521.

Fan, H.T., Shi, L.Q., Shen, H., Chen, X., Xie, K.P., 2016. Equilibrium, isotherm, kinetic and thermodynamic studies for removal of tetracycline antibiotics by adsorption onto hazelnut shell derived activated carbons from aqueous media. RSC Adv. 6, 109983–109991.

Fazal, M.A., Kawachi, T., Ichion, E., 2001. Extent and severity of groundwater arsenic contamination in Bangladesh. Water Int. 26, 370–379.

Finocchio, E., Lodi, A., Solisio, C., Converti, A., 2010. Chromium (VI) removal by methylated biomass of *Spirulina platensis*: the effect of methylation process. Chem. Eng. J. 156 (2), 264–269.

Foroutan, R., Peighambardoust, S.J., Aghdasinia, H., Mohammadi, R., Ramavandi, B., 2020. Modification of bio-hydroxyapatite generated from waste poultry bone with MgO for purifying methyl violet-laden liquids. Environ. Sci. Pollut. Control Ser. 1–12.

Foroutan, R., Peighambardoust, S.J., Ahmadi, A., Akbari, A., Farjadfard, S., Ramavandi, B., 2021a. Adsorption mercury, cobalt, and nickel with a reclaimable and magnetic composite of hydroxyapatite/Fe$_3$O$_4$/polydopamine. J. Environ. Chem. Eng. 1–11.

Foroutan, R., Mohammadi, R., Ahmadi, A., Bikhabar, G., Babaei, F., Ramavandi, B., 2022. Impact of ZnO and Fe$_3$O$_4$ magnetic nanoscale on the methyl violet 2B removal efficiency of the activated carbon oak wood. Chemosphere 1–13.

Foroutan, R., Peighambardoust, S.J., Hemmati, S., Ahmadi, A., Falletta, E., Ramavandi, B., 2021b. Zn$^{2+}$ removal from the aqueous environment using a polydopamine/hydroxyapatite/Fe$_3$O$_4$ magnetic composite under ultrasonic waves. RSC Adv. 27309–27321.

Foroutan, R., Peighambardoust, S.J., Latifi, P., Ahmadi, A., Alizadeh, M., Ramavandi, B., 2021c. Carbon nanotubes/β-cyclodextrin/MnFe$_2$O$_4$ as a magnetic nanocomposite powder for tetracycline antibiotic decontamination from different aqueous environments. J. Environ. Chem. Eng. 1–49.

Foroutan, R., Peighambardoust, S.J., Peighambardoust, S.H., Pateiro, M., Lorenzo, J., 2021d. Adsorption of crystal violet dye using activated carbon of lemon wood and activated carbon/Fe$_3$O$_4$ magnetic nanocomposite from aqueous solutions: a kinetic, equilibrium and thermodynamic study. J. Mol. 1–19.

Gadd, G.M., 1990. Heavy metal accumulation by bacteria and other microorganisms. Cell. Mol. Life Sci. 46, 834–840.

Gaur, N., Kukreja, A., Yadav, M., Tiwari, A., 2018. Adsorptive removal of lead and arsenic from aqueous solution using soya bean as a novel biosorbent: equilibrium isotherm and thermal stability studies. Appl. Water Sci. 1–12.

Ghayedi, N., Borazjani, J.M., Jafari, D., 2019. Biosorption of arsenic ions from the aqueous solutions using *Chlorella vulgaris* micro algae. Desalination Water Treat. 188–196.

Godlewska, k., Marycs, k., Izabela, M., 2018. Freshwater green macroalgae as abiosorbent of Cr (III) ions. De Gruyter 16, 689–701.

Hammouda, O., Abdel-Raouf, N., Shaaban, M., Kamal, M., Plant, B.S.W.T., 2015. Treatment of mixed domestic-industrial wastewater using microalgae *Chlorella sp.* Am. J. Sci. 11 (12), 303–315.

Hao, L., Liu, M., Wang, N., Li, G., 2018. A critical review on arsenic removal from water using iron-based adsorbents. R. Soc. Chem. 8, 39545–39560.

Ibrahim, W.M., Hassan, A.F., Azab, Y.A., 2016. Biosorption of toxic heavy metals from aqueous solution by *ulva lactuca* activated carbon. Egypt. J. Basic Appl. Sci. 3, 241–249.

Jaishankar, M., Tseten, T., Anbalagan, N., Mathew, B.B., Beeregowda, K.N., 2014. Toxicity, mechanism and health effects of some heavy metals. Interdiscipl. Toxicol. 7 (2), 60–72.

Jin, Y., Wang, X., Zang, T., Hu, Y., Hu, X., Ren, G., Xu, X., Qu, J., 2016. Biosorption of lead(II) by *Arthrobacter* sp. 25: process optimization and mechanism. J. Microbiol. Biotechnol. 26 (8), 1428–1438.

Kahraman, S., Hamamci, D.A., Erdemoglu, S., Yesilada, O., 2005. Biosorption of copper(II) by live and dried biomass of the. Eng. Life Sci. 5 (1), 72–77.

Kamble, P., Cheriyamundath, S., Lopus, M., Sirisha, V.L., 2018. Chemical characteristics, antioxidant and anticancer potential of sulfated polysaccharides from *Chlamydomonas reinhardtii*. J. Appl. Phycol. 30 (3), 1641–1653.

Kanamarlapudi, S.R., Muddada, S., 2019. Structural changes of *bacillus subtilis* biomass on biosorption of iron (II) from aqueous solutions: isotherm and Kinetic Studies. Pol. J. Microbiol. 68, 549–558.

Kashyap, M., Samadhiya, K., Ghosh, A., Anand, V., Shirage, P.M., Bala, K., 2019. Screening of microalgae for biosynthesis and optimization of Ag/AgCl nano hybrids having antibacterial effect. R. Soc. Chem. (44), 25583–25591.

Khajavian, M., Wood, D.A., Hallajsani, A., Majidian, N., 2019. Simultaneous biosorption of nickel and cadmium by the brown algae *Cystoseria indica* characterized by isotherm and kinetic models. KSABC 62–69.

Korake, S.R., Jadhao, P.D., 2021. Investigation of Taguchi optimization, equilibrium isotherms, and kinetic modeling for cadmium adsorption onto deposited silt. Heliyon, e05755.

Kumar, M., Singh, A.K., Sikandar, M., 2020. Biosorption of Hg (II) from aqueous solution using algal biomass: kinetics and isotherm studies. Heliyon 6 (1), e03321.

Kumar, K.S., Dahms, H.U., Won, E.J., Lee, J.S., Shin, K.H., 2015. Microalgae–A promising tool for heavy metal remediation. Ecotoxicol. Environ. Saf. 113, 329–352.

Ladeira, A.C.Q., Ciminelli, V.S.T., 2004. Adsorption and desorption of arsenic on an oxisol and its constituents. Water Res. 38, 2087–2094.

Lestari, I., Sy, S., Harmiwati, Kurniawati, D., Alif, A., Zein, R., Aziz, H., 2016. Effect of pH on the Biosorption of Heavy Metal by Alginate Immobilized Durian (Durio Zibethinus) Seed. Der Pharma Chemica, pp. 294–300.

Liao, D., Zheng, W., Li, X., Yang, Q., Yue, X., Guo, L., 2010. Removal of lead(II) from aqueous solutions using carbonate hydroxyapatite extracted from eggshell waste. J. Hazard Mater. 126–130.

Lim, J., Kang, H.M., Kim, L.H., ko, S.O., 2008. Removal of heavy metals by sawdust adsorption: equilibrium and kinetic studies. Kor. Soc. Environ. Eng. 13 (2), 79–84.

Long1, M., Jiang, H., Li, X., 2021. Biosorption of $Cu^{2+}$, $Pb^{2+}$, $Cd^{2+}$ and their mixture from aqueous solutions by Michelia figo sawdust. Sci. Rep. 1–12.

Machineni, L., 2019. Review on biological wastewater treatment and resources recovery: attached and suspended growth system. Water Sci. Technol. 20, 521–539.

Maisarah, Adityosulindro, S., Wulandari, D., 2021. Utilization of wild algae biomass as biosorbent for removal of heavy metal Zinc ($Zn^{2+}$) from aqueous. IOP Conf. Ser. Earth Environ. Sci. 20–27.

Malkoc, E., Nuhoglu, Y., 2003. The removal of chromium (VI) from synthetic wastewater by Ulothrix zonata. Fresenius Environ. Bull. 12, 376–381.

Mittal, A., Kurup, L., Mittal, J., 2007. Freundlich and Langmuir adsorption isotherms and kinetics for the removal of tartrazine from aqueous solutions using hen feathers. J. Hazard Mater. 243–248.

Mohkami, A., Pirkoohi, M.H., 2019. Arsenic removal from aqueous media using scenedesmus obliquus: the promoting impact of microalgae-bacteria consortium. J. Phycol. Res. 3 (1), 301–311.

Mohamad, A.M.N., Mat, D.W.S., Ismail, D., 2015. Fourier transform infrared (FTIR) spectroscopy with chemometric techniques for the classification of ballpoint pen inks. Arab J. Forensic Sci. Forensic Med. 1 (2), 194–200.

Mohamed, M.G., Hanaa, S.E.-D., Khalid, M.E.-M., Amer, A., Emad, H.A.-N., Lamiaa, I.M., 2014. Removal of cadmium from aqueous solution using marine green algae, Ulva lactuca. Egypt. J. Aquat. Res. 1–9.

Moghadam, M.R., Fatemi, S., Keshtkar, A., 2013. Adsorption of lead ($Pb^{2+}$) and uranium ($UO^{22+}$) cations by brown algae; experimental and thermodynamic modeling. Chem. Eng. J. 231–294.

Mosaferi, M., Nemati, S., Khataee, A., Nasseri, S., Hashemi, A.A., 2014. Removal of arsenic (III, V) from aqueous solution by nanoscale zero -valent iron stabilized with starch and carboxymethyl cellulose. J. Environ. Health Sci. Eng. 12–74.

Naeimi, B., Foroutan, R., Ahmadi, B., Sadeghzadeh, F., Ramavandi, B., 2018. Pb(II) and Cd(II) removal from aqueous solution, shipyard wastewater, and landfill leachate by modified Rhizopus oryzae biomass. Mater. Res. Express 1–30.

Nalenthiran, Pugazhenthiran, Sambandam, Anandan, Ashokkumar, Muthupandian, 2016. Removal of Heavy Metal from Wastewater, pp. 1–27.

Obulapuram, P.K., Arfin, T., Mohammad, F., Khiste, S.K., Chavali, M., Albalawi, A.N., Al-Lohedan, H.A., 2021. Adsorption, equilibrium isotherm, and thermodynamic studies towards the removal of reactive orange 16 dye Cu(I)-Polyaniline composite. J. Polym. Sci. 13, 1–16.

Olukanni, D.O., Agunwamba, J.C., Ugwu, E.I., 2014. Biosorption of heavy metals in industrial wastewater using micro-organisms Pseudomonas aeruginosa. Am. J. Sci. Ind. Res. 5 (2), 81–87.

Patiha, E.H., Hidayat, Y., Firdaus, M., 2016. The Langmuir isotherm adsorption equation: the monolayer approach. 10th Joint Conference on Chemistry. IOP Conf. Ser. Mater. Sci. Eng. 107 (2016), 012067.

Peighambardoust, S.J., Foroutan, R., Peighambardoust, S.H., Khatooni, H., Ramavandi, B., 2021. Decoration of Citrus limon wood carbon with $Fe_3O_4$ to enhanced $Cd^{2+}$ removal: a reclaimable and magnetic nanocomposite. Chemosphere 1–10.

Petrovic, A., Simonic, M., 2016. Removal of heavy metal ions from drinking water by alginate-immobilised Chlorella sorokiniana. Int. J. Environ. Sci. Technol. 13, 1761–1780.

Piasecka, A., Cieśla, J., Koczańska, M., Krzemińska, I., 2019. Effectiveness of Parachlorella kessleri cell disruption evaluated with the use of laser light scattering methods. J. Appl. Phycol. 31, 97–107.

Rippka, R., 1988. Recognition and identification of cyanobacteria. Methods Enzymol. 16, 28–67.

Sarada, B., Prasad, M.K., Kumar, K.K., Murthy, C.R., 2017. Biosorption of $Cd^{+2}$ by green plant biomass, araucaria heterophylla: characterization, kinetic, isotherm and thermodynamic studies. Appl. Water Sci. 7, 3483–3496.

Satya, A., Harimawan, A., Haryani, G.S., Johir, M.A., Vigneswaran, S., Ngo, H.H., Setiadi, T., 2020. Batch study of cadmium biosorption by carbon dioxide enriched aphanothece sp. dried biomass. MDPI 12 (1), 1–19.

Savari, A., Hashemi, S., Arfaeinia, H., Dobaradaran, S., Froutan, R., Mahvi, A.H., 2020. Physicochemical characteristics and mechanism of fluoride removal using powdered zeolite-zirconium in modes of pulsed& continuous sonication and stirring. Adv. Powder Technol. 1–11.

Savvidou, M.G., Dardavila, M.M., Georgiopoulou, I., Louli, V., Stamatis, H., Kekos, D., Voutsas, E., 2021. Optimization of microalga Chlorella vulgaris magnetic harvesting. Nanomaterials 11, 1–18.

Seo, H., Lee, M., Wang, S., 2013. Equilibrium and kinetic studies of the biosorption of dissolved metals on bacillus drentensis immobilized in biocarrier beads. Environ. Eng. Res. 18 (1), 45–53.

Sibi, G., 2014. Biosorption of arsenic by living and dried biomass of fresh water microalgae - potentials and equilibrium studies. J. Biorem. Biodegrad. (2155-6199), 1–8.

Singh, J.S., Kumar, A., Rai, A.N., Singh, D.P., 2016. Cyanobacteria: a precious bio-resource in agriculture, ecosystem, and environmental sustainability. Front. Microbiol. 7 (529), 1–19.

Spain, O., Plöhn, M., Funk, h., 2020. The cell wall of green microalgae and its role in heavy metal removal. Physiol. Plantarum 526–535.

Sreedhar, I., Reddy, N.S., 2019. Heavy Metal Removal from Industrial Effluent Using Bio Sorbent Blends. Springer Nature, pp. 1–15.

Tchounwou, P.B., Yedjou, C.G., Patlolla, A.K., Sutton, D.J., 2012. Heavy metal toxicity and the environment. Experientia Suppl. 2012 (101), 133–164.

Tounsadi, H., Khalidi, A., Abdennouri, M., Barka, N., 2015. Biosorption potential of Diplotaxis harra and Glebionis coronaria L.biomasses for the removal of Cd (II) and Co (II) from aqueous solutions. J. Environ. Chem. Eng. 3, 822–830.

Ubando, A.T., Africa, A.D.M., Maniquiz-Redillas, M.C., Culaba, A.B., Chen, W.H., Chang, J.S., 2020. Microalgal biosorption of heavy metals: a comprehensive bibliometric review. J. Hazard Mater. 402, 123431. 1–123431.11.

Veera, M.B., Abburi, K., Jonathan, L.T., Edgar, D.S., Haasch, R., 2008. Removal of arsenic (III) and arsenic (V) from aqueous medium using chitosan-coated biosorbent. sciencedirect 42, 633–642.

Vogel, M., et al., 2010. Biosorption of U (VI) by the green algae Chlorella vulgaris independence of pH value and cell activity. Sci. Total Environ. 409, 384–395.

Yogeshwaran, V., Priya, K.A., 2022. Biosorption of heavy metal ions from the aqueous solutions using porous Sargassum Wightii SWbrown algae: batch adsorption, kinetic and thermodynamic studies. Res. Square 1–32.

Zand, A.D., Abyaneh, M.R., 2020. Adsorption of lead, manganese, and copper onto biochar in landfill leachate:implication of non-linear regression analysis. Res. Square 1–16.

Zeraatkar, A.K., Ahmadzadeh, H., Talebi, A.F., Moheimani, N.R., McHenry, M.P., 2016. Potential use of algae for heavy metal bioremediation, a critical review. J. Environ. Manag. 181, 817–831.